

1 **Dysregulation of the Tweak/Fn14 pathway in skeletal muscle of spinal muscular atrophy mice**

2

3 Katharina E. Meijboom ^{1,2}, Emily McFall ³, Daniel Anthony ⁴, Benjamin Edwards ¹, Sabrina Kubinski ⁵,
4 Gareth Hazell ¹, Nina Ahlskog ^{1,7}, Peter Claus ^{5,6}, Kay E. Davies ¹, Rashmi Kothary ³, Matthew J.A. Wood
5 ^{1,7}, Melissa Bowerman ^{1,8,9*}

6

7 ¹ Department of Physiology, Anatomy and Genetics, University of Oxford, Oxford, United Kingdom

8 ² Gene Therapy Center, UMass Medical School, Worcester, United States.

9 ³ Ottawa Hospital Research Institute, Regenerative Medicine Program, Ottawa, Canada and; Department of
10 Cellular and Molecular Medicine, University of Ottawa, Ottawa, Canada.

11 ⁴ Department of Pharmacology, University of Oxford, Oxford, United Kingdom.

12 ⁵ Institute of Neuroanatomy and Cell Biology, Hannover Medical School, Hannover, Germany and; Center
13 for Systems Neuroscience, Hannover, Germany.

14 ⁶ SMATHERIA – Non-Profit Biomedical Research Institute, Hannover, Germany.

15 ⁷ Department of Paediatrics, University of Oxford, Oxford, United Kingdom.

16 ⁸ School of Medicine, Keele University, Staffordshire, United Kingdom.

17 ⁹ Wolfson Centre for Inherited Neuromuscular Disease, RJA Orthopaedic Hospital, Oswestry, United
18 Kingdom.

19

20 * Corresponding author: m.bowerman@keele.ac.uk

21

22 **ABSTRACT**

23 Spinal muscular atrophy (SMA) is a childhood neuromuscular disorder caused by depletion of the survival
24 motor neuron (SMN) protein. SMA is characterized by the selective death of spinal cord motor neurons,
25 leading to progressive muscle wasting. Loss of skeletal muscle in SMA is a combination of denervation-
26 induced muscle atrophy and intrinsic muscle pathologies. Elucidation of the pathways involved is essential
27 to identify the key molecules that contribute to and sustain muscle pathology. The tumor necrosis factor-like
28 weak inducer of apoptosis (TWEAK)/TNF receptor superfamily member fibroblast growth factor inducible
29 14 (Fn14) pathway has been shown to play a critical role in the regulation of denervation-induced muscle
30 atrophy as well as muscle proliferation, differentiation and metabolism in adults. However, it is not clear
31 whether this pathway would be important in highly dynamic and developing muscle. We thus investigated
32 the potential role of the TWEAK/Fn14 pathway in SMA muscle pathology, using the severe Taiwanese *Smn*
33 $^{/-};SMN2$ and the less severe $Smn^{2B/-}$ SMA mice, which undergo a progressive neuromuscular decline in the
34 first three post-natal weeks. Here, we report significantly dysregulated expression of the TWEAK/Fn14
35 pathway during disease progression in skeletal muscle of the two SMA mouse models. In addition, siRNA-
36 mediated *Smn* knockdown in C2C12 myoblasts suggests a genetic interaction between *Smn* and the
37 TWEAK/Fn14 pathway. Further analyses of SMA, *Tweak* $^{/-}$ and *Fn14* $^{/-}$ mice revealed dysregulated
38 myopathy, myogenesis and glucose metabolism pathways as a common skeletal muscle feature, and
39 providing further evidence in support of a relationship between the TWEAK/Fn14 pathway and *Smn*.
40 Finally, a pharmacological intervention (Fc-TWEAK) to upregulate the activity of the TWEAK/Fn14
41 pathway improved disease phenotypes in the two SMA mouse models. Our study provides novel mechanistic
42 insights into the molecular players that contribute to muscle pathology in SMA and into the role of the
43 TWEAK/Fn14 pathway in developing muscle.

44 **Keywords:** spinal muscular atrophy, survival motor neuron, *Smn*, *Tweak*, *Fn14*, glucose metabolism,
45 skeletal muscle, atrophy, denervation

47 **BACKGROUND**

48 The neuromuscular disease spinal muscular atrophy (SMA) is the leading genetic cause of infant mortality
49 [1]. SMA is caused by mutations in the *survival motor neuron 1 (SMN1)* gene [2]. The major pathological
50 components of SMA pathogenesis are the selective loss of spinal cord alpha motor neurons and muscle
51 wasting [3]. Skeletal muscle pathology is a clear contributor to SMA disease manifestation and progression
52 and is caused by both denervation-induced muscle atrophy [4,5] and intrinsic defects [6–8]. As skeletal
53 muscle is the largest insulin-sensitive tissue in the body and is involved in glucose utilization [9], it is not
54 surprising that muscle metabolism is also affected in SMA. Impaired metabolism has indeed been reported
55 in SMA Type 1, 2 and 3 patients [10–14]. A better understanding of the specific molecular effectors that
56 contribute to SMA muscle physiopathology could provide mechanistic insights in SMA muscle pathology
57 and help therapeutic endeavors aimed at improving muscle health in patients [15].

58

59 One pathway that plays a crucial role in chronic injury and muscle diseases is the tumor necrosis factor-like
60 weak inducer of apoptosis (TWEAK) and its main signaling receptor, the TNF receptor superfamily member
61 fibroblast growth factor inducible 14 (Fn14) [16–18]. TWEAK is ubiquitously expressed and synthesized as
62 a Type II transmembrane protein but can also be cleaved by proteolytic processing and secreted as a soluble
63 cytokine [19]. The role of the TWEAK/Fn14 pathway in skeletal muscle is conflicting as it has been
64 demonstrated to have both beneficial and detrimental effects on muscle health and function [20,21]. Indeed,
65 pathologically high levels of TWEAK activate the canonical nuclear factor kappa-light-chain-enhancer of
66 activated B cells (NF- κ B) pathway, which promotes myoblast proliferation and thus inhibits myogenesis and
67 the early phases of muscle repair and regeneration [22,23]. Conversely, lower physiological concentrations
68 of TWEAK activate the non-canonical NF- κ B pathway that promotes myoblast fusion and myogenesis [24].
69 The transmembrane protein Fn14 is typically dormant or present in low levels in normal healthy muscle
70 [25]. Atrophic inducing conditions (e.g. casting and surgical denervation) stimulate the expression of Fn14,
71 leading to the chronic activation of the TWEAK/Fn14 pathway and sustained skeletal muscle atrophy [26].

72 We have also demonstrated an increased activity of the Tweak/Fn14 pathway in skeletal muscle of a mouse
73 model of the neurodegenerative adult disorder amyotrophic lateral sclerosis (ALS), which is characterized
74 by a progressive and chronic denervation-induced muscle atrophy [27]. In addition, various downstream
75 effectors of the TWEAK/Fn14 pathway play critical roles in the regulation of muscle metabolism such as
76 peroxisome proliferator-activated receptor-gamma coactivator 1 α (PGC-1 α), glucose transporter 4 (Glut-4),
77 myogenic transcription factor 2d (Mef2d), hexokinase II (HKII) and Krüppel-like factor 15 (Klf15) [28–34].
78

79 Although the TWEAK/Fn14 pathway has been ascribed roles in both skeletal muscle health regulation and
80 metabolism, both of which are impacted in SMA [35,36], this pathway has yet to be investigated in the
81 context of SMA. Furthermore, all research on this pathway has been performed in adult mice and therefore
82 has never been explored in early phases of muscle development. We thus investigated the potential role of
83 TWEAK/Fn14 signaling in SMA and in early phases of post-natal skeletal muscle development. We report
84 significantly decreased levels of both *Tweak* and *Fn14* during disease progression in two distinct SMA
85 mouse models (*Smn*^{-/-};SMN2 and *Smn*^{2B/-}) [37,38]. We also observed dysregulated expression of *PGC-1 α* ,
86 *Glut-4*, *Mef2d* and *HKII*, the metabolic downstream effectors of TWEAK/Fn14 signaling [29,30], in skeletal
87 muscle of these SMA mice. In addition, more in-depth analyses revealed an overlap of aberrantly expressed
88 genes that regulate myopathy, myogenesis and glucose metabolism pathways in skeletal muscle of SMA,
89 *Tweak*^{-/-} and *Fn14*^{-/-} mice, further supporting shared functions between the TWEAK/Fn14 pathway and SMN
90 in developing muscle. Finally, upregulation of the activity of the TWEAK/Fn14 pathway, through a
91 pharmacological intervention (Fc-TWEAK administration), improved disease phenotypes in the two SMA
92 mouse models. Our study uncovers novel mechanistic insights into the molecular effectors that contribute to
93 skeletal muscle pathology in SMA and demonstrates a role for the TWEAK/Fn14 pathway in the early stages
94 of post-natal muscle development.

95

96

97 **METHODS**

98 Animals and animal procedures

99 Wild-type mice FVB/N [39] and C57BL/6J [40] and the severe *Smn*^{-/-};SMN2 mouse model (FVB.Cg-
100 *Smn1tm1Hung* Tg(SMN2)2Hung/J) [41] were obtained from Jackson Laboratories. The *Smn*^{2B/-} mouse
101 model [38,42] was kindly provided by Dr. Lyndsay M Murray (University of Edinburgh). *Tweak*^{-/-} [43] and
102 *Fn14*^{-/-} mouse models [44] were generously obtained from Linda C. Burkly (Biogen).

103 Most experiments with live animals were performed at the Biomedical Services Building, University of
104 Oxford. Experimental procedures were authorized and approved by the University of Oxford ethics
105 committee and UK Home Office (current project license PDFEDC6F0, previous project license 30/2907) in
106 accordance with the Animals (Scientific Procedures) Act 1986. Experiments with the *Smn*^{2B/-} mice in Figure
107 1 were performed at the University of Ottawa Animal Facility according to procedures authorized by the
108 Canadian Council on Animal Care.

109 Fc-TWEAK was administered by subcutaneous injections using a sterile 0.1 cc insulin syringe at various
110 doses (7.9 µg, 15.8 µg or 31.6 µg) and at a volume of 20 µl either daily, every other day or every four days.
111 Mouse Fc-TWEAK, a fusion protein with the murine IgG2a Fc region, and Ig isotope control were kindly
112 provided by Linda C. Burkly (Biogen) [43].

113 For survival studies, mice were weighed and monitored daily and culled upon reaching their defined humane
114 endpoint.

115 For all experiments, litters were randomly assigned at birth and whole litters composed of both sexes were
116 used. Sample sizes were determined based on similar studies with SMA mice.

117 To reduce the total number of mice used, the fast-twitch tibialis anterior (TA) and triceps muscles from the
118 same mice were used interchangeably for respective molecular and histological analyses.

119

120

121

122 Sciatic nerve crush

123 For nerve crush experiments, post-natal day (P) 7 wild-type (WT) FVB/N mice [39] were anesthetized with
124 2% isoflurane/oxygen before one of their lateral thighs was shaved and a 1 cm incision in the skin was made
125 over the lateral femur. The muscle layers were split with blunt scissors, the sciatic nerve localized and
126 crushed with tweezers for 15 seconds. The skin incision was closed with surgical glue and animals allowed
127 to recover on a warming blanket. Ipsilateral and contralateral TA muscles were harvested at P14 and either
128 fixed in 4% paraformaldehyde (PFA) for 24 hours for histological analyses or snap frozen for molecular
129 analyses.

130

131 Cardiotoxin injections

132 Cardiotoxin γ (Cytotoxin I, Latoxan, L8102, Portes les Valence) was dissolved in 0.9% saline and injected
133 4 μ l/g per total mouse weight of a 10 μ M solution into the left TA muscle of WT FVB/N mice [39] at post-
134 natal day (P) 10. The right TA was injected with equal volumes of 0.9% saline. During the injection, mice
135 were anesthetized with 2% isoflurane/oxygen and all injections were done using a sterile 0.3 cc insulin
136 syringe. TA muscles were harvested 6 days later and either fixed in 4% PFA for 24 hours for histological
137 analyses or snap frozen for molecular analyses.

138

139 Laminin staining of skeletal muscle

140 TA muscles were fixed in PFA overnight. Tissues were sectioned (13 μ m) and incubated in blocking buffer
141 for 2 hours (0.3% Triton-X, 20% fetal bovine serum (FBS) and 20% normal goat serum in PBS). After
142 blocking, tissues were stained overnight at 4°C with rat anti-laminin (1:1000, Sigma L0663) in blocking
143 buffer. The next day, tissues were washed in PBS and probed using a goat-anti-rat IgG 488 secondary
144 antibody (1:500, Invitrogen A-11006) for one hour. PBS-washed tissues were mounted in Fluoromount-G
145 (Southern Biotech). Images were taken with a DM IRB microscope (Leica) with a 20X objective.
146 Quantitative assays were performed blinded on 3-5 mice for each group and five sections per mouse. The

147 area of muscle fiber within designated regions of the TA muscle sections was measured using Fiji (ImageJ)
148 [45].

149

150 Hematoxylin and eosin staining of skeletal muscle

151 TA muscles were fixated in 4% PFA and imbedded into paraffin blocks. For staining, muscles were sectioned
152 (13 μ m) and deparaffinized in xylene and then fixed in 100% ethanol. Following a rinse in water, samples
153 were stained in hematoxylin (Fisher) for 3 minutes, rinsed in water, dipped 40 times in a solution of 0.02%
154 HCl in 70% ethanol and rinsed in water again. The sections were next stained in a 1% eosin solution (BDH)
155 for 1 minute, dehydrated in ethanol, cleared in xylene, and mounted with Fluoromount-G (Southern Biotech).
156 Images were taken with a DM IRB microscope (Leica) with a 20X objective. Quantitative assays were
157 performed blinded on 3-5 mice for each group and five sections per mouse. The area of muscle fibre within
158 designated regions of the TA muscle sections was measured using Fiji (ImageJ) [45].

159

160 Cell culture

161 Both C2C12 myoblasts [46] and NSC-34 neuronal-like cells [47] were maintained in growth media
162 consisting of Dulbecco's Modified Eagle's Media (DMEM) supplemented with 10% FBS and 1%
163 Penicillin/Streptomycin (all Life Technologies). Cells were cultured at 37°C with 5% CO₂. C2C12 myoblasts
164 were differentiated in DMEM containing 2% horse serum for 7 days to form multinucleated myotubes.
165 Cells were regularly tested for mycoplasma and remained mycoplasma-free.

166

167 In vitro siRNA knockdown

168 For small interfering RNA (siRNA) transfections, C2C12 myoblasts were seeded onto 12-well plates at a
169 50% confluency and cultured overnight in 2 mL of DMEM. Cells were washed with PBS prior to siRNA
170 transfection, whereby 100 pmol of each siRNA (*Tweak*, *Fn14*, *Smn*) (Invitrogen, assay IDs s233937,
171 s203164, s74017, respectively) in a complex with 10 μ l of Lipofectamine RNAiMAX (Invitrogen) dissolved

172 in OptiMEM solution (Gibco) was added to the cells for three hours. The transfection mix was then
173 substituted either for DMEM without the siRNAs for 1 day or with a differentiation medium mix without
174 the siRNAs for 7 days.

175

176 **qPCR**

177 RNA was extracted from tissues and cells either by a RNeasy kit from Qiagen or by guanidinium
178 thiocyanate-acid-phenol-chloroform extraction using TRIzol Reagent (Life Technologies) as per
179 manufacturer's instructions. The same RNA extraction method was employed for similar experiments and
180 equal RNA amounts were used between samples within the same experiments. cDNA was prepared with the
181 High Capacity cDNA Kit (Life Technologies) according to the manufacturer's instructions. The cDNA
182 template was amplified on a StepOnePlus Real-Time PCR Thermocycler (Life Technologies) with SYBR
183 Green Mastermix from Applied Biosystems. qPCR data was analyzed using the StepOne Software v2.3
184 (Applied Biosystems). Primers used for qPCR were obtained from IDT and sequences for primers were
185 either self-designed or ready-made (Supplementary Table 1). Relative gene expression was quantified using
186 the Pfaffl method [48] and primer efficiencies were calculated with the LinRegPCR software. We
187 normalized relative expression level of all tested genes in mouse tissue and cells to *RNA polymerase II*
188 *polypeptide J (PolJ)* [49].

189

190 **PCR array**

191 RNA was extracted using the RNeasy® Microarray Tissue Kit (Qiagen). cDNA was generated with the RT²
192 First Strand Kit (Qiagen). qPCRs were performed using RT² Profiler™ PCR Array Mouse Skeletal Muscle:
193 Myogenesis & Myopathy Mouse (PAMM-099Z, SABiosciences) and RT² Profiler™ PCR Array Mouse
194 Glucose Metabolism (PAMM-006Z SABiosciences). The data were analyzed with RT Profiler PCR Array
195 Data Analysis (version 3.5) and mRNA expression was normalized to the two most stably expressed genes
196 between all samples. We used the publicly available database STRING (version 10.5) for network and

197 enrichment analysis of differently expressed genes [50]. The minimum required interaction score was set at
198 0.4, medium confidence.

199

200 Western blot

201 Freshly prepared radioimmunoprecipitation (RIPA) buffer was used to homogenize tissue and cells,
202 consisting of 50 mM Tris pH 8.8, 150mM NaCl, 1% NP-40, 0.5% sodium deoxycholate, 0.1% SDS and
203 complete mini-proteinase inhibitors (Roche). Equal amounts of total protein were loaded, as measured by
204 Bradford Assay. Protein samples were first diluted 1:1 with Laemmli sample buffer (Bio-Rad, Hemel
205 Hempstead, UK) containing 5% β -mercaptoethanol (Sigma) and heated at 100°C for 10 minutes. Next,
206 samples were loaded on freshly made 1.5 mm 12% polyacrylamide separating and 5% stacking gel and
207 electrophoresis was performed at 120 V for ~1.5 hours in running buffer. Subsequently, proteins were
208 transferred from the gel onto to a polyvinylidene fluoride membrane (Merck Millipore) via electroblotting
209 at 120 V for 60 minutes in transfer buffer containing 20% methanol. Membranes were then incubated for 2
210 hours in Odyssey Blocking Buffer (Licor). The membrane was then probed overnight at 4°C with primary
211 antibodies (P105/p50, 1:1000, Abcam ab32360; Actin, 1:1000, Abcam ab3280) in Odyssey Blocking Buffer
212 and 0.1% Tween-20. The next day, after three 10-minute washing steps with PBS, the membrane was
213 incubated for 1 hour at room temperature with secondary antibodies (goat anti-rabbit IgG 680RD, 1:1000,
214 LI-COR 926-68071; goat anti-mouse IgG 800CW, 1:1000 LI-COR, 926-32210). Lastly, the membrane was
215 washed three times for 10 minutes in PBS and visualized by scanning 700 nm and 800 nm channels on the
216 LI-COR Odyssey CLx infrared imaging system (LI-COR) for 2.5 minutes per channel. The background was
217 subtracted and signal of protein of interest was divided by signal of the housekeeping protein.

218

219 Statistical Analysis

220 All statistical analyses were done with the most up to date GraphPad Prism software. When appropriate, a
221 Student's unpaired two-tail *t*-test, a one-way ANOVA or a two-way ANOVA was used. *Post-hoc* analyses

222 used are specified in Figure Legends. Outliers were identified via the Grubbs' test. For the Kaplan-Meier
223 survival analysis, the log-rank test was used and survival curves were considered significantly different at
224 $p<0.05$.

225

226

227

228

229

230

231

232

233

234

235

236

237

238

239

240

241 **RESULTS**

242 **The TWEAK/Fn14 pathway is dysregulated in two SMA mouse models**

243 We firstly investigated the expression of the TWEAK/Fn14 pathway in skeletal muscle of the severe
244 Taiwanese *Smn*^{-/-};SMN2 mouse model [37], using muscles with reported differential vulnerability to
245 neuromuscular junction (NMJ) denervation (vulnerability: triceps brachii > gastrocnemius > TA >
246 quadriceps femoris) [51]. Muscles were harvested from *Smn*^{-/-};SMN2 and WT mice at several time points
247 during disease progression: birth (post-natal day (P) 0, pre-symptomatic (P2), early symptomatic (P5), late-
248 symptomatic (P7) and end stage (P10)).

249

250 We assessed the expression of *parvalbumin*, a high affinity Ca²⁺-binding protein, which is downregulated in
251 denervated muscle [52,53] and a marker of muscle atrophy in skeletal muscle of SMA patients and
252 *Smn*^{-/-};SMN2 mice [54]. We observed a significant decreased expression of *parvalbumin* mRNA during
253 disease progression (Fig. 1a) in SMA mice compared to WT animals, further confirming parvalbumin as a
254 *bona fide* marker of muscle atrophy in SMA [54]. Furthermore, we noted that parvalbumin expression was
255 downregulated at earlier time points in the two most vulnerable muscles (triceps and gastrocnemius) [51] of
256 SMA mice compared to WT animals (Fig. 1a).

257

258 We next evaluated the expression of *Tweak* and *Fn14* and observed significant decreased levels of *Tweak*
259 mRNA in muscles of *Smn*^{-/-};SMN2 mice during disease progression, except in the quadriceps (Fig. 1b), in
260 accordance with it being a relatively invulnerable SMA muscle [51]. Similarly, we found significantly lower
261 levels of *Fn14* mRNA in all muscles of *Smn*^{-/-};SMN2 mice during disease progression (Fig. 1c) compared to
262 WT animals. Interestingly, the decreased expression of *Fn14* in denervated and atrophied muscles of
263 neonatal animals is different to previous reports in adults where denervation-induced atrophy stimulates its
264 expression [26,27].

265

266 As mentioned above, the TWEAK/Fn14 pathway has been reported to negatively regulate the expression of
267 metabolic effectors Klf15, Pgc-1 α , Mef2d, Glut-4 and HKII [29]. Given that we have previously published
268 a concordant increased expression of *Klf15* in skeletal muscle of SMA mice during disease progression [55],
269 we next evaluated if the additional downstream metabolic targets were similarly dysregulated in the
270 predicted directions. We indeed observed that the mRNA expression of *Pgc-1 α* , *Mef2d*, *Glut-4* and *HKII*
271 was significantly upregulated in muscles of *Smn*^{-/-};SMN2 mice at symptomatic time-points (P5-P10)
272 compared to WT animals (Fig. 1d-g), showing an expected opposite pattern to both *Tweak* and *Fn14* (Fig.
273 1b-c) [29]. Notably, we also found that in most muscles, mRNA levels of *Pgc-1 α* , *Mef2d*, *Glut4* and *HKII*
274 were significantly decreased in pre-symptomatic *Smn*^{-/-};SMN2 mice (P0-P5) compared to WT animals (Fig.
275 1d-g), independently of *Tweak* and *Fn14* (Fig. 1b-c).
276

277 TWEAK/Fn14 pathway also regulates the canonical and non-canonical NF- κ B pathways in skeletal muscle
278 [56,57]. In pre-symptomatic (P2) TA muscle, we observed no significant difference in the expression of NF-
279 κ B1 (p50), a component of the canonical NF- κ B pathway, between *Smn*^{-/-};SMN2 mice and WT animals (Fig.
280 1h), consistent with normal *Tweak* and *Fn14* levels (Fig. 1b-c). Conversely, there was a significant decreased
281 expression of NF- κ B1 (p50) in TA muscle of symptomatic *Smn*^{-/-};SMN2 mice compared to WT animals at
282 P7 (Fig. 1i), in line with reduced levels of *Tweak* and *Fn14* (Fig. 1b). We also investigated the expression of
283 NF- κ B-inducing kinase (NIK), involved in the non-canonical NF- κ B activation pathway [58]. We observed
284 that mRNA levels of NIK were significantly increased in TA muscle of P7 *Smn*^{-/-};SMN2 mice compared to
285 WT animals (Fig. 1j), suggesting that dysregulated activity of the Tweak/Fn14 in skeletal muscle of SMA
286 mice impacts both the canonical and non-canonical NF- κ B pathways, which play key regulatory roles in
287 muscle health and metabolism [20,21].
288

289 Finally, we evaluated the expression of the TWEAK/Fn14 signaling cascade in skeletal muscle of the less
290 severe *Smn*^{2B/-} mouse model of SMA [38]. TA muscles were harvested from *Smn*^{2B/-} mice and age-matched

291 WT animals at P0 (birth), P2 (early pre-symptomatic), P4 (late pre-symptomatic), P11 (early symptomatic)
292 and P19 (end stage). We found a significant decreased expression of *parvalbumin* (Fig. 1k), *Tweak* (Fig. 1l)
293 and *Fn14* (Fig. 1m) in muscle from *Smn^{2B/-}* mice during disease progression compared to WT animals,
294 similar to that observed in the more severe *Smn^{-/-};SMN2* SMA mouse model (Fig. 1a-c). We have previously
295 reported the aberrant increased expression of *Klf15* in the TA muscle of *Smn^{2B/-}* mice during disease
296 progression [55]. However, we did not observe an increase in expression of *Pgc-1α* (Fig. 1n), *Mef2d* (Fig
297 1o), *Glut-4* (Fig 1p) and *HKII* (Fig. 1q), suggesting that the negative regulation of these downstream
298 metabolic effectors may be dependent on disease severity, age and/or genetic strain.

299

300 We have thus demonstrated that the TWEAK/Fn14 pathway is dysregulated during progressive muscle
301 atrophy in two SMA mouse models.

302

303 **Denervation does not affect the Tweak/Fn14 pathway during the early stages of muscle development**

304 As SMA muscle pathology is defined by both intrinsic defects and denervation-induced events, we set out
305 to determine which of these may influence the dysregulation of the Tweak/Fn14 pathway in SMA muscle.
306 We firstly addressed the denervation component by performing nerve crush experiments in which the sciatic
307 nerves of P7 WT mice were crushed and the muscle harvested at P14 [59]. Of note, the sciatic nerve was
308 crushed in only one hindlimb, leaving the other control hindlimb intact. Quantification of myofiber area in
309 TA muscles showed a significant decrease in myofiber size in the nerve crush muscle compared to the control
310 hindlimb (Fig. 2a-c).

311

312 Expression analyses further revealed that there were no significant changes in mRNA levels of *parvalbumin*,
313 *Tweak*, *Fn14*, *PGC-1α*, *Mefd2*, *Glut-4* and *HKII* in the denervated muscle compared to the control TA
314 muscle (Fig. 2d). Interestingly, while denervation in adult muscle induces a dramatic surge in Fn14
315 expression [26,27], this did not occur in the denervated muscles of our pre-weaned mice, suggesting an age

316 and/or development regulatory element to this response. We also investigated the expression of *Klf15* and
317 *Smn* and similarly observed no significant differences between the nerve crush and control muscles (Fig.
318 2d).

319

320 Overall, these results suggest that the dysregulation of parvalbumin and the Tweak/Fn14 pathway in SMA
321 muscle during disease progression is most likely not denervation-dependent.

322

323 **Intrinsic muscle injury affects the Tweak/Fn14 pathway during the early stages of muscle
324 development**

325 We next investigated what impact impairing intrinsic muscle integrity would have on the Tweak/Fn14
326 pathway. To do so, we used cardiotoxin to induce myofiber necrosis. Cardiotoxin was injected in P10 WT
327 mice into the left TA while the right TA was injected with equal volumes of 0.9% saline and used as a control
328 [60]. TAs were harvested after 6 days, a time-point where muscles are still in an immature and regenerating
329 mode [61]. Indeed, analysis of centrally located nuclei showed a significantly increased percentage of
330 regenerating myofibers in cardiotoxin-treated muscles compared to saline-treated TAs (Fig. 3a-b).

331

332 We then proceeded with molecular analyses and observed that the atrophy marker *parvalbumin* was
333 significantly downregulated in cardiotoxin-treated TA muscles compared to saline-treated TA muscles (Fig.
334 3c). *Fn14* mRNA expression was significantly increased after cardiotoxin injury, in accordance with
335 previous research showing that muscle damage conditions activate Fn14 [26]. Conversely, *Pgc-1 α* , *Glut-4*,
336 *HKII* and *Klf15* mRNA levels were significantly downregulated (Fig. 3c), supporting their reported negative
337 regulation by the Tweak/Fn14 pathway [29]. Interestingly, *Tweak* mRNA expression remained unchanged,
338 contrary to reports of upregulation following cardiotoxin injury in adult muscle [62], suggesting a differential
339 response in early developmental stages of skeletal muscle. Notably, *Smn* expression was significantly

340 increased in the regenerating muscles compared to saline-treated TA muscles (Fig. 3c), perhaps due to
341 SMN's role during muscle fiber regeneration [63].

342

343 Together, these results demonstrate that intrinsic muscle injury in pre-weaned mice induces a dysregulation
344 of the Tweak/Fn14 signaling cascade. However, the changes were in the opposite direction than that
345 observed in SMA muscles (Fig. 1b), perhaps due to the necrosis and regeneration events that occur following
346 cardiotoxin injury [64], which are not typically found in muscles of SMA mice.

347

348 **Genetic interactions between *Smn*, Tweak and Fn14 in muscle**

349 We next wanted to further understand the potential relationship between dysregulated expression of *Tweak*,
350 *Fn14* and *Smn* in skeletal muscle of SMA mice. To do so, we evaluated the impact of Tweak and Fn14
351 depletion in the early stages of muscle development by performing molecular analyses on P7 triceps from
352 *Fn14*^{-/-} [44], *Tweak*^{-/-} [43] and WT mice. In *Tweak*^{-/-} mice, we observed a significant increased expression
353 of *Fn14* with a concomitant significantly decreased expression of *Klf15* compared to WT animals (Fig. 4a).

354 Notably, we found a significant decreased expression of *Smn* in *Tweak*^{-/-} triceps compared to WT mice (Fig.
355 4a), suggesting a direct or indirect positive interaction between Tweak and Smn levels. For their part,
356 *Fn14*^{-/-} mice displayed a significant downregulation of *parvalbumin* and a significant upregulation of *Pgc-*
357 *Iα* (Fig. 4b). These analyses further validate the reported negative regulation of *Pgc-1α* and *Klf15* by Fn14
358 and support the absence of overt pathological muscle phenotypes in young *Tweak*^{-/-} and *Fn14*^{-/-} mice [26,65].

359

360 To further dissect the relationship between Smn and the Tweak/Fn14 pathway during myogenic
361 differentiation, we performed siRNA-mediated knockdown of *Smn*, *Tweak* and *Fn14* in C2C12 myoblasts
362 and evaluated the effect on the Tweak/Fn14 signaling in undifferentiated (Day 0) and differentiated (Day 7)
363 cells. Reduced levels of *Smn*, *Tweak* and *Fn14* were significantly maintained in both proliferating and
364 differentiated cells following transfection with *siSmn*, *siTweak* and *siFn14*, respectively (Fig. 4c-e). We

365 observed an interaction between *Smn*, *Tweak* and *Fn14* specifically in differentiated C2C12s, whereby *Smn*
366 expression was significantly upregulated in *Fn14*-depleted D7 cells (Fig. 4c), *Tweak* expression was
367 significantly reduced in *Smn*-depleted D7 cells (Fig. 4d), and *Fn14* levels were significantly decreased in
368 *Tweak*- and *Smn*-depleted D7 cells (Fig. 4e). Similarly, the effects of siRNA-mediated knockdown of *Smn*,
369 *Tweak* and *Fn14* on downstream metabolic effectors were only apparent in differentiated C2C12s (Fig. 4f-
370 j). Indeed, both knockdown of *Tweak* and *Fn14* resulted in a significant upregulation of *Pgc-1α* (Fig. 4f) and
371 *Mef2d* (Fig. 4g). While *Glut-4* expression was neither affected by depletion of *Smn*, *Tweak* or *Fn14* (Fig.
372 4h), *HKII* mRNA levels were significantly decreased following knockdown of all three (Fig. 4i). Finally,
373 *Klf15* expression was significantly increased in siRNA-mediated knockdown of *Fn14* only (Fig. 4j). The
374 upregulation of *Pgc-1α*, *Mef2d*, and *Klf15* in *Tweak*- and/or *Fn14*-depleted differentiated C2C12 cells is in
375 accordance with the previously reported negative regulation of these genes by the Tweak/Fn14 pathway
376 while the unchanged *Glut-4* and downregulated *HKII* levels were not [18].

377

378 Thus, using both *in vivo* and *in vitro* models, we have thus provided evidence for a potential interaction
379 between *Smn*, *Tweak* and *Fn14* and subsequent impact on the Tweak/Fn14 signaling cascade (Fig. 4k). Our
380 results suggest that the aberrant expression of the Tweak/Fn14 pathway in SMA muscle during disease
381 progression may be due to a dynamic interplay between atrophic conditions and the molecular impact,
382 individual and combined, of reduced expression of *Smn*, *Tweak* and *Fn14* in the early developmental stages
383 of skeletal muscle.

384

385 **Overlap of dysregulated myopathy and myogenesis genes and glucose metabolism genes in SMA,
386 *Fn14*^{-/-} and *Tweak*^{-/-} mice**

387 To further decipher the potential contribution(s) of *Smn*, *Tweak* and *Fn14* depletion to SMA muscle
388 pathology, we used commercially available mouse myopathy and myogenesis qPCR arrays
389 (SABiosciences), which measure expression levels of a subset of 84 genes known to display and/or regulate

390 myopathy and myogenesis. We used triceps (vulnerable) and quadriceps (resistant) from P7 *Smn*^{-/-};*SMN2*,
391 *Tweak*^{-/-}, *Fn14*^{-/-} mice. WT FVB/N mice were compared to SMA animals and WT C57BL/6 mice were
392 compared to *Tweak*^{-/-} and *Fn14*^{-/-} mice to account for differences due to genetic strains. Unsurprisingly, we
393 observed a larger number of significantly dysregulated myopathy and myogenesis genes in triceps of
394 *Smn*^{-/-};*SMN2* mice than in the more resistant quadriceps, some of which overlapped with the subset of genes
395 aberrantly expressed in *Fn14*^{-/-} mice and *Tweak*^{-/-} mice (Fig. 5a, Table 1, Supplementary File 1). We also
396 used the publicly available database STRING [50] to perform network and enrichment analysis of the shared
397 differently expressed genes in both triceps and quadriceps (Table 1), which revealed that there were no
398 known protein-protein interactions between any of the dysregulated genes and Smn, Fn14 or Tweak (Fig.
399 5b). Interestingly, the central connectors *Myod1* and *Myf6* were upregulated and *Pax7* was downregulated
400 in the triceps of all three experimental groups (Table 1). *Myod1* and *Myf6* are key myogenic regulatory
401 factors (MRFs) and are normally upregulated after skeletal muscle injury [66]. *Pax7* is a canonical marker
402 for satellite cells, the resident skeletal muscle stem cells [66], and reduced activity of *Pax7* leads to cell-
403 cycle arrest of satellite cells and dysregulation of MRFs in skeletal muscle [67]. Furthermore, *Titin* (*Ttn*)
404 was downregulated in the quadriceps muscles of all three mouse models and plays major roles in muscle
405 contraction and force production, highlighted by titin mutations leading to a range of skeletal muscle diseases
406 and phenotypes [68].

407

408 Next, as both SMA and the Tweak/Fn14 pathway have both been associated with glucose metabolism
409 abnormalities [29,69], we performed similar gene expression analyses with commercially available qPCR
410 arrays (SABiosciences) containing a subset of 84 genes known to display and/or regulate glucose
411 metabolism. We found a similar large number of genes that were dysregulated in both triceps and quadriceps
412 muscles of *Smn*^{-/-};*SMN2* mice, some of which overlapped with those differentially expressed in *Fn14*^{-/-} and
413 *Tweak*^{-/-} mice (Fig. 5c, Table 2, Supplementary File 2). STRING network and enrichment analysis [50]
414 revealed that there are no known protein-protein interactions between any of the dysregulated genes and

415 Smn, Fn14 or Tweak. Further analysis of Kyoto Encyclopedia of Genes and Genomes (KEGG) pathways
416 composed of the glucose metabolism genes significantly dysregulated in the same direction in triceps and
417 quadriceps muscles of P7 *Smn*^{-/-};SMN2, *Fn14*^{-/-} and *Tweak*^{-/-} mice as well as the downstream effectors of the
418 TWEAK/Fn14 pathway studied in this project (Pgc-1 α , Mef2d, Glut4, Klf15, and HKII) reveals that many
419 aspects of glucose metabolism, such as insulin signaling, glycolysis are dysregulated in Smn-, Tweak- and
420 Fn14-depleted mice (Table 3).

421

422 We thus show a shared pattern of aberrantly expressed genes that modulate myogenesis, myopathy and
423 glucose metabolism in SMA, Tweak-depleted and Fn14-depleted skeletal muscle, suggesting that Smn and
424 the Tweak/Fn14 pathway may act synergistically on muscle pathology and metabolism defects in SMA
425 muscle.

426

427 **Increasing Tweak activity improves a subset of disease phenotypes in two SMA mouse models**

428 Finally, we evaluated the impact of activating the Tweak/Fn14 pathway on disease progression and muscle
429 pathology in SMA mice. To do so, *Smn*^{-/-};SMN2 mice and healthy littermates received a daily subcutaneous
430 injection of Fc-TWEAK (15.8 μ g), a fusion protein with the murine IgG2a Fc region [43], starting at birth.
431 We found that Fc-TWEAK did not significantly impact weight or survival of *Smn*^{-/-};SMN2 mice compared
432 to untreated and IgG-treated controls (Fig. 6a-b). Additional lower (7.9 μ g) and higher doses (23 and 31.6
433 μ g) were also administered but proved to negatively impact weight and survival (Supplementary Fig. 1).

434

435 Triceps from P7 untreated and Fc-TWEAK-treated (15.8 μ g) *Smn*^{-/-};SMN2 SMA mice and *Smn*^{+/+};SMN2
436 healthy littermates were further processed for molecular analyses of the Tweak/Fn14 pathway. We observed
437 that Fc-TWEAK administration did not influence the expression of *Tweak* (Fig. 6c) or *Fn14* (Fig. 6d) in
438 neither *Smn*^{+/+};SMN2 nor *Smn*^{-/-};SMN2 mice compared to untreated animals. Accordingly, Fc-TWEAK did
439 not induce changes in *Pgc-1 α* expression (Fig. 6e). We did observe a significant downregulation of *Mef2d*

440 in Fc-TWEAK-treated muscles of *Smn*^{+/−};SMN2 SMA mice compared to untreated animals (Fig. 6f). *Glut-4*
441 mRNA expression remained unchanged in both *Smn*^{+/−};SMN2 and *Smn*^{+/−};SMN2 Fc-TWEAK-treated mice
442 (Fig. 6g). *HKII* was significantly upregulated in muscle of Fc-TWEAK-treated *Smn*^{+/−};SMN2 healthy
443 littermates while it was significantly downregulated in Fc-TWEAK-treated *Smn*^{+/−};SMN2 SMA mice
444 compared to untreated groups (Fig. 6h). *Klf15* was significantly downregulated in Fc-treated *Smn*^{+/−};SMN2
445 SMA only compared to untreated SMA animals (Fig. 6i). The absence of overt changes in the expression of
446 Tweak, Fn14 and downstream metabolic effectors may be due to the 24 hour time-lapse between the last Fc-
447 Tweak injection and harvest of tissues, which could have led to missing key time-points at which
448 transcriptional profiles were significantly impacted.

449

450 Whilst we did not capture the short-term molecular effects of Fc-TWEAK administration, quantification of
451 myofiber area in TA muscles showed that daily Fc-TWEAK treatment significantly increased myofiber area
452 in skeletal muscle of P7 *Smn*^{+/−};SMN2 mice compared to untreated SMA animals (Fig. 6j-l). Furthermore, the
453 expression of atrophy markers *parvalbumin*, *MuRF-1* and *atrogin-1* [70] was also restored towards normal
454 levels, whereby *parvalbumin* expression was significantly increased (Fig. 6m) whilst *MuRF-1* and *atrogin-1*
455 expression was significantly downregulated (Fig. 6n-o) in triceps of Fc-TWEAK-treated *Smn*^{+/−};SMN2
456 SMA mice compared to untreated SMA animals, further supporting an improvement in muscle health. We
457 did not however detect changes in MRFs *Myod1* and *myogenin* [66] (Fig. 6p-r).

458

459 We next assessed the effect of Fc-TWEAK in *Smn*^{2B/−} mice, which are typically more responsive to Smn-
460 independent treatment strategies [55,71–73]. Due to the longer treatment period in these mice (20 days) and
461 the observed toxicity in daily injected mice (> 10 days), the *Smn*^{2B/−} and *Smn*^{2B/+} mice received subcutaneous
462 injections of Fc-TWEAK and IgG control (15.8 µg) every 4 days, starting at birth. Both IgG and Fc-TWEAK
463 did not significantly impact the weight of *Smn*^{2B/−} mice compared to untreated SMA animals (Fig. 6s).
464 However, Fc-TWEAK significantly increased the lifespan of *Smn*^{2B/−} mice compared to both IgG-treated

465 and untreated animals (Fig. 6t). Molecular analyses of triceps from P15 animals only showed a significant
466 effect of Fc-TWEAK on the expression of *Glut-4*, whereby it was downregulated in Fc-TWEAK-treated
467 *Smn*^{2B/-} mice compared to untreated animals (Fig. 6u). Similarly to above, the limited impact of Fc-TWEAK
468 on the expression of the Tweak/Fn14 signaling cascade is most likely due to the 72-hour time-lapse between
469 the last injection of Fc-Tweak and tissue harvest.

470

471 Taken together, our results demonstrate that increasing Tweak activity in SMA mice has the potential to
472 improve weight, survival, and muscle pathology, suggesting that restoring the Tweak/Fn14 pathway in SMA
473 muscle may lead to sustainable therapeutic benefits.

474

475

476

477

478

479

480

481

482

483

484

485

486

487

488

489

490

491 **DISCUSSION**

492 Motor neuron death and muscle pathology bi-directionally impact on each other in SMA. Indeed, while loss
493 of motor neurons significantly contributes to muscle atrophy, there is also evidence for muscle-intrinsic
494 abnormalities in SMA skeletal muscle, which could be directly or indirectly caused by SMN deficiency [6–
495 8,74,75]. In this study, we addressed the underlying mechanisms of muscle-intrinsic abnormalities leading
496 to muscle pathology in SMA by investigating the role of the TWEAK/Fn14 pathway in muscle atrophy in
497 SMA. To the best of our knowledge, this is the first study to evaluate the TWEAK/Fn14 pathway in SMA
498 and in early stages of muscle development.

499

500 Notably, we showed decreased expression of *Tweak* and *Fn14* in skeletal muscle of two distinct SMA mouse
501 models during disease progression, which is contrary to previous reports of increased TWEAK/Fn14 activity
502 in experimental models of atrophy in adult muscle [18,76,77], suggesting that the TWEAK/Fn14 pathway
503 may have distinct roles in skeletal muscle during development and adulthood. Indeed, *Tweak* mRNA
504 expression is significantly lower in skeletal muscle of 30-day-old WT mice compared to 90-day-old animals,
505 suggesting an age-dependent regulation [78]. Moreover, we observed that the dysregulation of the
506 TWEAK/Fn14 pathway in skeletal muscle of pre-weaned mice appears to be influenced by intrinsic
507 myopathy and not denervation, which is in contrast to what has been reported in experimental models of
508 adult muscle denervation [26,27], further suggesting distinct developmental roles for the Tweak/Fn14
509 pathway in skeletal muscle. Given that muscles from younger mice are more resistant to surgically-induced
510 denervation than in older mice [79], the TWEAK/Fn14 pathway may contribute to this age-dependent
511 differential vulnerability of muscle to pathological insults. Thus, the role of TWEAK/Fn14 signaling in
512 muscle pathology may be more nuanced and be influenced by a combination of factors such as absolute
513 levels, downstream signaling cascades activated (e.g. canonical vs non-canonical NF-κB signaling
514 pathways), developmental stage of the muscle, state of muscle atrophy (e.g. chronic vs acute) and primary
515 origin of muscle pathology (e.g. denervation vs intrinsic insult) [20,21].

516 Another key observation from our study is a potential interaction and/or overlap between Tweak, Fn14 and
517 Smn and their downstream signaling cascades in muscle. It has previously been demonstrated that once
518 Tweak binds to Fn14, the complex will activate several NF- κ B molecular effectors, including TRAF6 and
519 IKK [80]. Interestingly, SMN has been reported to prevent the activation of TRAF6 and IKK, thereby
520 negatively regulating the muscle atrophy-inducing canonical NF- κ B pathway [81]. These studies thus
521 suggest converging roles for TWEAK, Fn14 and Smn in muscle, which is further supported by our findings.
522 Indeed, we found that independent *Tweak*, *Fn14* and *Smn* depletion had an impact on each other's expression
523 in differentiated C2C12 cells and murine muscle. Furthermore, there was an overlap of dysregulated
524 myogenesis, myopathy and glucose metabolism genes in SMA, *Fn14*^{-/-} and *Tweak*^{-/-} mice. Thus, these results
525 suggest that aberrant expression of the TWEAK/Fn14 pathway in SMA muscle may be a consequence of
526 combined events resulting from muscle atrophy events and reduced SMN expression.

527
528 In addition, our results in developing mice do support the previously reported negative regulation of the
529 metabolic factors Pgc-1 α , Mef2d, Glut4, Klf15, and HKII in adult muscle [29]. Further analyses of a subset
530 of specific glucose metabolism genes showed that about 20% of these genes were dysregulated in the same
531 direction in *Fn14*^{-/-}, TWEAK^{-/-} and SMA mice. Our KEGG analysis of these shared dysregulated metabolic
532 genes further support the potential relationships and roles of TWEAK, Fn14 and SMN involved in the
533 regulation of glucose metabolism. Indeed, the AMPK signaling pathway, found to be aberrantly regulated
534 in *Fn14*^{-/-}, TWEAK^{-/-} and SMA, is as a master regulator of skeletal muscle function and metabolism [82].
535 Interestingly, a previous study in *SMN* Δ 7 SMA mice further showed that chronic treatment with the AMPK
536 agonist AICAR prevented skeletal muscle pathology [83]. In addition, AMPK directly phosphorylates PGC-
537 1 α [84], which is also dysregulated in *Smn*-, *Tweak*- and *Fn14*-depleted models [85,86]. We also found that
538 glycolysis and pyruvate metabolic pathways, which culminate in the generation of ATP, are also
539 dysregulated in SMA, *Fn14*^{-/-} and *Tweak*^{-/-} mice. Interestingly, siRNA-mediated *Smn* knockdown in NSC-
540 34 cells showed a significant decrease in ATP production [87]. ATP was also decreased in *Smn*^{-/-};SMN2 mice

541 and in *Smn* morphant zebrafish [88]. These results could explain mitochondrial dysfunction in SMA patients
542 [7]. Thus, our study strengthens the notion of metabolic dysfunctions contributing to SMA muscle pathology
543 and suggests a potential mechanistic link with the TWEAK/Fn14 pathway.

544

545 Our findings also confirm that not all skeletal muscles are equally affected in SMA. Indeed, we observed
546 that the SMA skeletal muscle atrophy marker *parvalbumin* was significantly decreased from an earlier
547 timepoint in the vulnerable triceps and gastrocnemius muscles than in the more resistant TA and quadriceps
548 muscles. Notably, we also found that 20% more myogenesis- and myopathy-related genes were dysregulated
549 in the more vulnerable triceps muscles of *Smn*^{-/-};SMN2 mice compared to the resistant quadriceps muscles.
550 Conversely, the number of glucose metabolism genes dysregulated in SMA triceps and quadriceps muscles
551 was not significantly different. Previous studies have reported that muscle vulnerability is more closely
552 associated with NMJ denervation than with location or fibre type composition [51]. Our results further
553 suggest that denervation events in vulnerable SMA muscles have a more prominent effect on myogenesis
554 and myopathy than on glucose metabolism.

555

556 Finally, modulating Tweak activity via Fc-TWEAK in two SMA mouse models led to interesting
557 observations. Firstly, Fc-TWEAK administration specifically increased lifespan in the milder *Smn*^{2B/-} mouse
558 model while it did not impact disease progression in the severe *Smn*^{-/-};SMN2 mice. This is consistent with
559 previous studies, including ours, demonstrating that the *Smn*^{2B/-} mice are more responsive to non-SMN
560 treatments, perhaps due to their longer asymptomatic, and therefore adaptable period [55,71–73,89]. At a
561 molecular level, we found that Fc-Tweak differentially impacted the expression of the *Tweak*, *Fn14* and their
562 metabolic effectors in SMA mice and healthy littermates, perhaps reflecting disease-state dependent
563 regulatory mechanisms of the pathway. Importantly, the expression of *Mef2d*, *HKII* and *Klf15* was
564 significantly downregulated in Fc-TWEAK-treated SMA mice, supporting an increased activity of Tweak
565 in the mice and a subsequent restoration towards normal levels of aberrantly regulated Tweak/Fn14 effectors.

566 As mentioned above, the timing between Fc-Tweak administration and tissue collection may have limited
567 our analysis of the effect of Fc-Tweak on the Tweak/Fn14 signaling cascade. Nevertheless, administration
568 of Fc-Tweak did improve muscle pathology in SMA mice as demonstrated by the partial restoration of
569 molecular markers of muscle health and myofiber size. These results support a role for the TWEAK/Fn14
570 pathway in maintaining skeletal muscle health and homeostasis [21]. However, it is important to note that
571 the TWEAK/Fn14 pathway is involved in many other tissues and pathologies such as tumor development
572 and metastasis, heart-related diseases [90], kidney injury, cerebral ischemia [91,92] and autoimmune
573 diseases [93,94], which could have influenced the overall impact of systemically administered Fc-Tweak on
574 muscle health and disease progression in SMA mice.

575

576

577

578

579

580

581

582

583

584

585

586

587

588

589

590

591 **CONCLUSION**

592

593 In summary, our results demonstrate a potential role and contribution of the TWEAK/Fn14 pathway to
594 myopathy and glucose metabolism perturbations in SMA muscle. Furthermore, our study, combined with
595 previous work in adult models [20,21], suggests that dysregulation of the TWEAK/Fn14 signaling in muscle
596 appears to be dependent on the origin of the muscle pathology (e.g. denervation vs intrinsic) and
597 developmental stage of skeletal muscle (e.g. newborn, juvenile, adult, aged), further highlighting the
598 differential and conflicting activities of the pathway. Future investigations should be aimed at both furthering
599 our understanding of the relevance of the Tweak/Fn14 pathway in SMA muscle and defining its role in
600 general in maintaining muscle homeostasis throughout the life course.

601

602

603 **LIST OF ABBREVIATIONS**

604	ALS	amyotrophic lateral sclerosis
605	ANOVA	analysis of variance
606	cDNA	complementary deoxyribonucleic acid
607	DEG	differently expressed genes
608	DMEM	Dulbecco's Modified Eagle's Media
609	FBS	fetal bovine serum
610	FDR	false discovery rate
611	GO	gene ontology
612	H&E	hematoxylin-and-eosin
613	KEGG	Kyoto Encyclopedia of Genes and Genomes
614	mRNA	messenger RNA
615	NF-κB	nuclear factor kappa-light-chain-enhancer of activated B cells
616	NMJ	neuromuscular junctions
617	P	postnatal day
618	<i>p</i>	probability value
619	PBS	phosphate buffered saline
620	PCR	polymerase chain reaction
621	PFA	paraformaldehyde
622	qPCR	quantitative polymerase chain reaction
623	RIPA	radioimmunoprecipitation
624	RNA	ribonucleic acid
625	RNAi	RNA interference
626	RT-qPCR	reverse transcriptase-quantitative PCR
627	SEM	standard error of the mean

628	siRNA	small interfering RNA
629	SMA	spinal muscular atrophy
630	STRING	Search Tool for the Retrieval of Interacting Genes/Proteins
631	TA	tibialis anterior
632	WT	wild type
633		
634		
635		

636 **DECLARATIONS**

637 **Ethics approval and consent to participate**

638 Most experiments with live animals were performed at the Biomedical Services Building, University of
639 Oxford. Experimental procedures were authorized and approved by the University of Oxford ethics
640 committee and UK Home Office (current project license PDFEDC6F0, previous project license 30/2907) in
641 accordance with the Animals (Scientific Procedures) Act 1986. Experiments with the *Smn*^{2B/-} mice in Figure
642 1 were performed at the University of Ottawa Animal Facility according to procedures authorized by the
643 Canadian Council on Animal Care.

644

645 **Consent for publication**

646 Not applicable.

647

648 **Availability of data and materials**

649 All data generated or analyzed during this study are included in this published article or in the supplementary
650 information.

651

652 **Competing interests**

653 The authors declare they have no competing interests.

654

655 **Funding**

656 K.E.M. was funded by the MDUK and SMA Trust (now SMA UK). M.B. was funded by the SMA Trust
657 (now SMA UK) and Muscular Dystrophy Ireland/MRCG-HRB (MRCG-2016-21). S.K. was supported by
658 an ERASMUS grant. P.C. received financial support from the Deutsche Muskelstiftung. R.K. was funded
659 by the Canadian Institutes of Health Research and Muscular Dystrophy Association (USA).

660

661 **Authors' contributions**

662 Conceptualization: M.B.; Methodology: K.E.M, M.B; Validation: K.E.M., M.B.; Formal analysis: K.E.M.,
663 E.M., S.K., M.B.; Investigations: K.E.M., E.M., D.A., B.E., S.K., G.H., N.A., M.B.; Writing - original draft
664 preparation: K.E.M, M.B.; Writing – review and editing: K.E.M., E.M., D.A., B.E., S.K., G.H., N.A., P.C.,
665 K.E.D., R.K., M.J.A.W., M.B.; Visualization: K.E.M., M.B.; Supervision: P.C., K.E.D., R.K., M.J.A.W.,
666 M.B.; Project administration: M.B.; Funding acquisition: R.K., M.J.A.W., M.B.

667

668 **Acknowledgements**

669 We would like to thank the staff at the BMS facility at the University of Oxford.

670

671

672 **REFERENCES**

673 1. Miniño AM, Xu J, Kochanek KD. National Vital Statistics Reports, Volume 59, Number 2, (December
674 9, 2010). 2008;

675 2. Lefebvre S, Bürglen L, Reboullet S, Clermont O, Burlet P, Viollet L, et al. Identification and
676 Characterization of a Spinal Muscular Atrophy-Determining Gene. *Cell*. 1995;80:155–65.

677 3. Crawford TO, Pardo CA. The neurobiology of childhood spinal muscular atrophy. *Neurobiol Dis*.
678 1996;3:97–110.

679 4. Swoboda KJ, Prior TW, Scott CB, McNaught TP, Wride MC, Reyna SP, et al. Natural History of
680 Denervation in SMA: Relation to Age, SMN2 Copy Number, and Function. *Ann Neurol*. 2005;57:704–12.

681 5. Torres-Benito L, Ruiz R, Tabares L. Synaptic defects in spinal muscular atrophy animal models. *Dev
682 Neurobiol*. 2012;72:126–33.

683 6. Rajendra TK, Gonsalvez GB, Walker MP, Shpargel KB, Salz HK, Matera AG. A *Drosophila melanogaster*
684 model of spinal muscular atrophy reveals a function for SMN in striated muscle. *J Cell Biol*. 2007;176:831–
685 41.

686 7. Ripolone M, Ronchi D, Violano R, Vallejo D, Fagiolari G, Barca E, et al. Impaired Muscle Mitochondrial
687 Biogenesis and Myogenesis in Spinal Muscular Atrophy. *JAMA Neurol*. NIH Public Access; 2015;72:666–
688 75.

689 8. Shafey D, Côté PD, Kothary R. Hypomorphic Smn knockdown C2C12 myoblasts reveal intrinsic defects
690 in myoblast fusion and myotube morphology. *Exp Cell Res*. Academic Press; 2005;311:49–61.

691 9. Stump CS, Henriksen EJ, Wei Y, Sowers JR. The metabolic syndrome: Role of skeletal muscle
692 metabolism. *Ann Med*. 2006;38:389–402.

693 10. Deguise M, Baranello G, Mastella C, Beauvais A, Michaud J, Leone A, et al. Abnormal fatty acid
694 metabolism is a core component of spinal muscular atrophy. *Ann Clin Transl Neurol.* 2019;6:1519–32.

695 11. Davis RH, Miller EA, Zhang RZ, Swoboda KJ. Responses to Fasting and Glucose Loading in a Cohort
696 of Well Children with Spinal Muscular Atrophy Type II. *J Pediatr.* 2015;167:1362-1368.e1.

697 12. Watson KS, Boukhloifi I, Bowerman M, Parson SH. The Relationship between Body Composition,
698 Fatty Acid Metabolism and Diet in Spinal Muscular Atrophy. *Brain Sci.* 2021;11.

699 13. Djordjevic SA, Milic-Rasic V, Brankovic V, Kosac A, Dejanovic-Djordjevic I, Markovic-Denic L, et al.
700 Glucose and lipid metabolism disorders in children and adolescents with spinal muscular atrophy types 2
701 and 3. *Neuromuscul Disord NMD.* 2021;

702 14. Li Y-J, Chen T-H, Wu Y-Z, Tseng Y-H. Metabolic and Nutritional Issues Associated with Spinal
703 Muscular Atrophy. *Nutrients.* 2020;12.

704 15. Boyer JG, Ferrier A, Kothary R. More than a bystander: the contributions of intrinsic skeletal muscle
705 defects in motor neuron diseases. *Front Physiol.* Frontiers Media SA; 2013;4:356.

706 16. Wiley SR, Winkles JA. TWEAK, a member of the TNF superfamily, is a multifunctional cytokine that
707 binds the TweakR/Fn14 receptor. *Cytokine Growth Factor Rev.* 14:241–9.

708 17. Tajrishi MM, Zheng TS, Burkly LC, Kumar A. The TWEAK-Fn14 pathway: a potent regulator of
709 skeletal muscle biology in health and disease. *Cytokine Growth Factor Rev.* 2014;25:215–25.

710 18. Shuichi Sato YOMMTAK, Sato S, Ogura Y, Tajrishi MM, Kumar A. Elevated levels of TWEAK in
711 skeletal muscle promote visceral obesity, insulin resistance, and metabolic dysfunction. *FASEB J Off Publ*
712 *Fed Am Soc Exp Biol.* The Federation of American Societies for Experimental Biology; 2015;29:988–1002.

713 19. Carmona Arana JA, Seher A, Neumann M, Lang I, Siegmund D, Wajant H. TNF Receptor-Associated
714 Factor 1 is a Major Target of Soluble TWEAK. *Front Immunol.* Frontiers Media SA; 2014;5:63.

715 20. Enwere EK, Lacasse EC, Adam NJ, Korneluk RG. Role of the TWEAK-Fn14-cIAP1-NF- κ B Signaling
716 Axis in the Regulation of Myogenesis and Muscle Homeostasis. *Front Immunol.* 2014;5:34.

717 21. Pascoe AL, Johnston AJ, Murphy RM. Controversies in TWEAK-Fn14 signaling in skeletal muscle
718 atrophy and regeneration. *Cell Mol Life Sci CMLS.* 2020;

719 22. Tidball JG, Villalta SA. Regulatory interactions between muscle and the immune system during muscle
720 regeneration. *Am J Physiol Regul Integr Comp Physiol.* 2010;298:R1173-87.

721 23. Merritt EK, Thalacker-Mercer A, Cross JM, Windham ST, Thomas SJ, Bamman MM. Increased
722 expression of atrogenes and TWEAK family members after severe burn injury in nonburned human skeletal
723 muscle. *J Burn Care Res Off Publ Am Burn Assoc.* 34:e297-304.

724 24. Enwere EK, Lacasse EC, Adam NJ, Korneluk RG. Role of the TWEAK-Fn14-cIAP1-NF- κ B Signaling
725 Axis in the Regulation of Myogenesis and Muscle Homeostasis. *Front Immunol.* 2014;5:34.

726 25. Meighan-Mantha RL, Hsu DK, Guo Y, Brown SA, Feng SL, Peifley KA, et al. The mitogen-inducible
727 Fn14 gene encodes a type I transmembrane protein that modulates fibroblast adhesion and migration. *J Biol
728 Chem.* 1999;274:33166–76.

729 26. Mittal A, Bhatnagar S, Kumar A, Lach-Trifilieff E, Wauters S, Li H, et al. The TWEAK-Fn14 system is
730 a critical regulator of denervation-induced skeletal muscle atrophy in mice. *J Cell Biol.* 2010;188:833–49.

731 27. Bowerman M, Salsac C, Coque E, Eiselt É, Deschaumes RG, Brodovitch A, et al. Tweak regulates
732 astrogliosis, microgliosis and skeletal muscle atrophy in a mouse model of amyotrophic lateral sclerosis.
733 *Hum Mol Genet.* 2015;24:3440–56.

734 28. Arany Z. PGC-1 coactivators and skeletal muscle adaptations in health and disease. *Curr Opin Genet*
735 *Dev.* 2008;18:426–34.

736 29. Sato S, Ogura Y, Tajirishi MM, Kumar A. Elevated levels of TWEAK in skeletal muscle promote visceral
737 obesity, insulin resistance, and metabolic dysfunction. *FASEB J Off Publ Fed Am Soc Exp Biol.*
738 2015;29:988–1002.

739 30. Sato S, Ogura Y, Kumar A. TWEAK/Fn14 Signaling Axis Mediates Skeletal Muscle Atrophy and
740 Metabolic Dysfunction. *Front Immunol.* 2014;5:18.

741 31. Klip A, McGraw TE, James DE. Thirty sweet years of GLUT4. *J Biol Chem.* 2019;294:11369–81.

742 32. Roberts DJ, Miyamoto S. Hexokinase II integrates energy metabolism and cellular protection: Akting
743 on mitochondria and TORCing to autophagy. *Cell Death Differ.* 2015;22:248–57.

744 33. Aziz A, Liu Q-C, Dilworth FJ. Regulating a master regulator: establishing tissue-specific gene expression
745 in skeletal muscle. *Epigenetics.* 2010;5:691–5.

746 34. Fan L, Hsieh PN, Sweet DR, Jain MK. Krüppel-like factor 15: Regulator of BCAA metabolism and
747 circadian protein rhythmicity. *Pharmacol Res.* 2018;130:123–6.

748 35. Wood MJA, Talbot K, Bowerman M. Spinal muscular atrophy: antisense oligonucleotide therapy opens
749 the door to an integrated therapeutic landscape. *Hum Mol Genet.* 2017;26:R151–9.

750 36. Boyer JG, Ferrier A, Kothary R. More than a bystander: the contributions of intrinsic skeletal muscle
751 defects in motor neuron diseases. *Front Physiol.* 2013;4:356.

752 37. Hsieh-Li HM, Chang JG, Jong YJ, Wu MH, Wang NM, Tsai CH, et al. A mouse model for spinal
753 muscular atrophy. *Nat Genet.* 2000;24:66–70.

754 38. Bowerman M, Murray LM, Beauvais A, Pinheiro B, Kothary R. A critical smn threshold in mice dictates
755 onset of an intermediate spinal muscular atrophy phenotype associated with a distinct neuromuscular
756 junction pathology. *Neuromuscul Disord NMD*. 2012;22:263–76.

757 39. Taketo M, Schroeder AC, Mobraaten LE, Gunning KB, Hanten G, Fox RR, et al. FVB/N: an inbred
758 mouse strain preferable for transgenic analyses. *Proc Natl Acad Sci U S A*. National Academy of Sciences;
759 1991;88:2065–9.

760 40. Mekada K, Abe K, Murakami A, Nakamura S, Nakata H, Moriwaki K, et al. Genetic differences among
761 C57BL/6 substrains. *Exp Anim*. 2009;58:141–9.

762 41. Hsieh-Li HM, Chang J-GG, Jong Y-JJ, Wu M-HH, Wang NM, Tsai CH, et al. A mouse model for spinal
763 muscular atrophy. *Nat Genet*. Nature Publishing Group; 2000;24:66–70.

764 42. Eshraghi M, McFall E, Gibeault S, Kothary R. Effect of genetic background on the phenotype of the
765 Smn2B/- mouse model of spinal muscular atrophy. *Hum Mol Genet*. 2016;25:4494–506.

766 43. Campbell S, Burkly LC, Gao H-X, Berman JW, Su L, Browning B, et al. Proinflammatory effects of
767 TWEAK/Fn14 interactions in glomerular mesangial cells. *J Immunol Baltim Md 1950*. 2006;176:1889–98.

768 44. Jakubowski A, Ambrose C, Parr M, Lincecum JM, Wang MZ, Zheng TS, et al. TWEAK induces liver
769 progenitor cell proliferation. *J Clin Invest*. 2005;115:2330–40.

770 45. Schindelin J, Arganda-Carreras I, Frise E, Kaynig V, Longair M, Pietzsch T, et al. Fiji: an open-source
771 platform for biological-image analysis. *Nat Methods*. Nature Publishing Group; 2012;9:676–82.

772 46. Yaffe D, Saxel O. Serial passaging and differentiation of myogenic cells isolated from dystrophic mouse
773 muscle. *Nature*. Nature Publishing Group; 1977;270:725–7.

774 47. Cashman NR, Durham HD, Blusztajn JK, Oda K, Tabira T, Shaw IT, et al. Neuroblastoma × spinal cord
775 (NSC) hybrid cell lines resemble developing motor neurons. *Dev Dyn.* 1992;194:209–21.

776 48. Pfaffl MW. A new mathematical model for relative quantification in real-time RT-PCR. *Nucleic Acids
777 Res.* Oxford University Press (OUP); 2001;29:45e–45.

778 49. Radonić A, Thulke S, Mackay IM, Landt O, Siegert W, Nitsche A. Guideline to reference gene selection
779 for quantitative real-time PCR. *Biochem Biophys Res Commun.* 2004;313:856–62.

780 50. Szklarczyk D, Morris JH, Cook H, Kuhn M, Wyder S, Simonovic M, et al. The STRING database in
781 2017: quality-controlled protein–protein association networks, made broadly accessible. *Nucleic Acids Res.*
782 2017;45:D362–8.

783 51. Ling KKY, Gibbs RM, Feng Z, Ko C-PC-P. Severe neuromuscular denervation of clinically relevant
784 muscles in a mouse model of spinal muscular atrophy. *Hum Mol Genet.* 2012;21:185–95.

785 52. Olive M, Ferrer I. Parvalbumin immunohistochemistry in denervated skeletal muscle. *Neuropathol Appl
786 Neurobiol.* 1994;20:495–500.

787 53. Müntener M, Berchtold MW, Heizmann CW. Parvalbumin in cross-reinnervated and denervated
788 muscles. *Muscle Nerve.* 1985;8:132–7.

789 54. Mutsaers CA, Wishart TM, Lamont DJ, Riessland M, Schreml J, Comley LH, et al. Reversible molecular
790 pathology of skeletal muscle in spinal muscular atrophy. *Hum Mol Genet.* 2011;20:4334–44.

791 55. Walter LM, Deguise M-O, Meijboom KE, Betts CA, Ahlskog N, van Westering TLE, et al. Interventions
792 Targeting Glucocorticoid-Krüppel-like Factor 15-Branched-Chain Amino Acid Signaling Improve Disease
793 Phenotypes in Spinal Muscular Atrophy Mice. *EBioMedicine.* 2018;31:226–42.

794 56. Li H, Mittal A, Paul PK, Kumar M, Srivastava DS, Tyagi SC, et al. Tumor Necrosis Factor-related Weak
795 Inducer of Apoptosis Augments Matrix Metalloproteinase 9 (MMP-9) Production in Skeletal Muscle
796 through the Activation of Nuclear Factor- κ B-inducing Kinase and p38 Mitogen-activated Protein Kinase.
797 *J Biol Chem.* 2009;284:4439–50.

798 57. Varfolomeev E, Goncharov T, Maecker H, Zobel K, Kömüves LG, Deshayes K, et al. Cellular inhibitors
799 of apoptosis are global regulators of NF- κ B and MAPK activation by members of the TNF family of
800 receptors. *Sci Signal.* 2012;5:ra22.

801 58. Li Y, Kang J, Friedman J, Tarassishin L, Ye J, Kovalenko A, et al. Identification of a cell protein (FIP-
802 3) as a modulator of NF- κ B activity and as a target of an adenovirus inhibitor of tumor necrosis factor -
803 induced apoptosis. *Proc Natl Acad Sci. National Academy of Sciences;* 1999;96:1042–7.

804 59. Magill CK, Tong A, Kawamura D, Hayashi A, Hunter DA, Parsadanian A, et al. Reinnervation of the
805 tibialis anterior following sciatic nerve crush injury: a confocal microscopic study in transgenic mice. *Exp
806 Neurol. NIH Public Access;* 2007;207:64–74.

807 60. McCullagh KJA, Edwards B, Kemp MW, Giles LC, Burgess M, Davies KE. Analysis of skeletal muscle
808 function in the C57BL6/SV129 syncoilin knockout mouse. *Mamm Genome.* 2008;19:339–51.

809 61. Yan Z, Choi S, Liu X, Zhang M, Schageman JJ, Lee SY, et al. Highly coordinated gene regulation in
810 mouse skeletal muscle regeneration. *J Biol Chem. American Society for Biochemistry and Molecular
811 Biology;* 2003;278:8826–36.

812 62. Mittal A, Bhatnagar S, Kumar A, Paul PK, Kuang S, Kumar A. Genetic ablation of TWEAK augments
813 regeneration and post-injury growth of skeletal muscle in mice. *Am J Pathol.* 2010;177:1732–42.

814 63. Kariya S, Obis T, Garone C, Akay T, Sera F, Iwata S, et al. Requirement of enhanced Survival
815 Motoneuron protein imposed during neuromuscular junction maturation. *J Clin Invest.* 2014;124:785–800.

816 64. Garry GA, Antony ML, Garry DJ. Cardiotoxin Induced Injury and Skeletal Muscle Regeneration. In:
817 Kyba M, editor. Skelet Muscle Regen Mouse Methods Protoc [Internet]. New York, NY: Springer; 2016
818 [cited 2020 May 28]. p. 61–71. Available from: https://doi.org/10.1007/978-1-4939-3810-0_6

819 65. Girgenrath M, Weng S, Kostek CA, Browning B, Wang M, Brown SAN, et al. TWEAK, via its receptor
820 Fn14, is a novel regulator of mesenchymal progenitor cells and skeletal muscle regeneration. *EMBO J.*
821 2006;25:5826–39.

822 66. Yin H, Price F, Rudnicki MA. Satellite Cells and the Muscle Stem Cell Niche. *Physiol Rev.* 2013;93:23–
823 67.

824 67. von Maltzahn J, Jones AE, Parks RJ, Rudnicki MA. Pax7 is critical for the normal function of satellite
825 cells in adult skeletal muscle. *Proc Natl Acad Sci U S A.* National Academy of Sciences; 2013;110:16474–
826 9.

827 68. Savarese M, Sarparanta J, Vihola A, Udd B, Hackman P. Increasing Role of Titin Mutations in
828 Neuromuscular Disorders. *J Neuromuscul Dis.* IOS Press; 2016;3:293–308.

829 69. Bowerman M, Swoboda KJ, Michalski J-P, Wang G-S, Reeks C, Beauvais A, et al. Glucose metabolism
830 and pancreatic defects in spinal muscular atrophy. *Ann Neurol.* 2012;72:256–68.

831 70. Bodine SC, Latres E, Baumhueter S, Lai VK, Nunez L, Clarke BA, et al. Identification of ubiquitin
832 ligases required for skeletal muscle atrophy. *Science.* American Association for the Advancement of
833 Science; 2001;294:1704–8.

834 71. Bowerman M, Beauvais A, Anderson CL, Kothary R. Rho-kinase inactivation prolongs survival of an
835 intermediate SMA mouse model. *Hum Mol Genet.* 2010;19:1468–78.

836 72. Kaifer KA, Villalón E, Osman EY, Glascock JJ, Arnold LL, Cornelison DDW, et al. Plastin-3 extends
837 survival and reduces severity in mouse models of spinal muscular atrophy. *JCI Insight*. 2017;2:e89970.

838 73. Osman EY, Rietz A, Kline RA, Cherry JJ, Hodgetts KJ, Lorson CL, et al. Intraperitoneal delivery of a
839 novel drug-like compound improves disease severity in severe and intermediate mouse models of Spinal
840 Muscular Atrophy. *Sci Rep*. 2019;9:1633.

841 74. Martínez-Hernández R, Soler-Botija C, Also E, Alias L, Caselles L, Gich I, et al. The developmental
842 pattern of myotubes in spinal muscular atrophy indicates prenatal delay of muscle maturation. *J Neuropathol
843 Exp Neurol*. Oxford University Press; 2009;68:474–81.

844 75. Martínez-Hernández R, Bernal S, Alias L, Tizzano EF. Abnormalities in Early Markers of Muscle
845 Involvement Support a Delay in Myogenesis in Spinal Muscular Atrophy. *J Neuropathol Exp Neurol*. Oxford
846 University Press; 2014;73:559–67.

847 76. Liu H, Peng H, Xiang H, Guo L, Chen R, Zhao S, et al. TWEAK/Fn14 promotes oxidative stress through
848 AMPK/PGC-1 α /MnSOD signaling pathway in endothelial cells. *Mol Med Rep*. Spandidos Publications;
849 2017;17:1998–2004.

850 77. Hindi SM, Mishra V, Bhatnagar S, Tajrishi MM, Ogura Y, Yan Z, et al. Regulatory circuitry of TWEAK-
851 Fn14 system and PGC-1 α in skeletal muscle atrophy program. *FASEB J Off Publ Fed Am Soc Exp Biol*.
852 2014;28:1398–411.

853 78. Bowerman M, Salsac C, Coque E, Eiselt E, Deschaumes RG, Brodovitch A, et al. Tweak regulates
854 astrogliosis, microgliosis and skeletal muscle atrophy in a mouse model of amyotrophic lateral sclerosis.
855 *Hum Mol Genet*. Oxford University Press; 2015;24:ddv094-.

856 79. Murray LM, Comley LH, Gillingwater TH, Parson SH. The response of neuromuscular junctions to
857 injury is developmentally regulated. *FASEB J*. 2011;25:1306–13.

858 80. Kumar A, Bhatnagar S, Paul PK. TWEAK and TRAF6 regulate skeletal muscle atrophy. *Curr Opin Clin*
859 *Nutr Metab Care. NIH Public Access*; 2012;15:233–9.

860 81. Kim EK, Choi E-J. SMN1 functions as a novel inhibitor for TRAF6-mediated NF- κ B signaling. *Biochim*
861 *Biophys Acta BBA - Mol Cell Res. Elsevier*; 2017;1864:760–70.

862 82. Kjøbsted R, Hingst JR, Fentz J, Foretz M, Sanz M-N, Pehmøller C, et al. AMPK in skeletal muscle
863 function and metabolism. *FASEB J Off Publ Fed Am Soc Exp Biol*. 2018;32:1741–77.

864 83. Cerveró C, Montull N, Tarabal O, Piedrafita L, Esquerda JE, Calderó J. Chronic Treatment with the
865 AMPK Agonist AICAR Prevents Skeletal Muscle Pathology but Fails to Improve Clinical Outcome in a
866 Mouse Model of Severe Spinal Muscular Atrophy. *Neurother J Am Soc Exp Neurother. Springer*;
867 2016;13:198–216.

868 84. Irrcher I, Ljubicic V, Kirwan AF, Hood DA. AMP-Activated Protein Kinase-Regulated Activation of
869 the PGC-1 α Promoter in Skeletal Muscle Cells. Lucia A, editor. *PLoS ONE*. 2008;3:e3614.

870 85. Hindi SM, Mishra V, Bhatnagar S, Tajrishi MM, Ogura Y, Yan Z, et al. Regulatory circuitry of TWEAK-
871 Fn14 system and PGC-1 α in skeletal muscle atrophy program. *FASEB J Off Publ Fed Am Soc Exp Biol*.
872 2014;28:1398–411.

873 86. Ng SY, Mikhail A, Ljubicic V. Mechanisms of exercise-induced survival motor neuron expression in
874 the skeletal muscle of spinal muscular atrophy-like mice. *J Physiol*. 2019;597:4757–78.

875 87. Acsadi G, Lee I, Li X, Khaidakov M, Pecinova A, Parker GC, et al. Mitochondrial dysfunction in a
876 neural cell model of spinal muscular atrophy. *J Neurosci Res*. 2009;87:2748–56.

877 88. Boyd PJ, Tu W-Y, Shorrock HK, Groen EJN, Carter RN, Powis RA, et al. Bioenergetic status modulates
878 motor neuron vulnerability and pathogenesis in a zebrafish model of spinal muscular atrophy. Cox GA,
879 editor. PLOS Genet. Public Library of Science; 2017;13:e1006744.

880 89. Bowerman M, Murray LM, Boyer JG, Anderson CL, Kothary R. Fasudil improves survival and promotes
881 skeletal muscle development in a mouse model of spinal muscular atrophy. BMC Med. 2012;10:24.

882 90. Jain M, Jakubowski A, Cui L, Shi J, Su L, Bauer M, et al. A Novel Role for Tumor Necrosis Factor-Like
883 Weak Inducer of Apoptosis (TWEAK) in the Development of Cardiac Dysfunction and Failure. Circulation.
884 2009;119:2058–68.

885 91. Inta I, Frauenknecht K, Dörr H, Kohlhof P, Rabsilber T, Auffarth GU, et al. Induction of the cytokine
886 TWEAK and its receptor Fn14 in ischemic stroke. J Neurol Sci. 2008;275:117–20.

887 92. Haile WB, Echeverry R, Wu F, Guzman J, An J, Wu J, et al. Tumor necrosis factor-like weak inducer of
888 apoptosis and fibroblast growth factor-inducible 14 mediate cerebral ischemia-induced poly(ADP-ribose)
889 polymerase-1 activation and neuronal death. Neuroscience. 2010;171:1256–64.

890 93. Yamana J, Morand EF, Manabu T, Sunahori K, Takasugi K, Makino H, et al. Inhibition of TNF-induced
891 IL-6 by the TWEAK-Fn14 interaction in rheumatoid arthritis fibroblast like synoviocytes. Cell Immunol.
892 2012;272:293–8.

893 94. El-shehaby A, Darweesh H, El-Khatib M, Momtaz M, Marzouk S, El-Shaarawy N, et al. Correlations of
894 Urinary Biomarkers, TNF-Like Weak Inducer of Apoptosis (TWEAK), Osteoprotegerin (OPG), Monocyte
895 Chemoattractant Protein-1 (MCP-1), and IL-8 with Lupus Nephritis. J Clin Immunol. 2011;31:848–56.

896

897

898

899

900

901

902

903

904

905

906

907

908 **FIGURE LEGENDS**

909 **Figure 1. Aberrant expression of the TWEAK/Fn14 signaling pathway in skeletal muscle of SMA mice.**

910 **a-g.** qPCR analysis of *parvalbumin* (**a**), *Tweak* (**b**), *Fn14* (**c**), *Pgc-1α* (**d**), *Mef2d* (**e**), *Glut-4* (**f**) and *HKII* (**g**)
911 in triceps, gastrocnemius, TA and quadriceps muscles from post-natal day (P) 0 (birth), P2 (pre-
912 symptomatic), P5 (early-symptomatic), P7 (late symptomatic) and P19 (end-stage) *Smn*^{-/-};SMN2 and wild
913 type (WT) mice. Data are mean ± SEM, n = 3-4 animals per experimental group, two-way ANOVA, Sidak's
914 multiple comparison test, * p < 0.05, ** p < 0.01, *** p < 0.001, **** p < 0.0001. **h-i.** Quantification of NF-
915 κB p50/actin protein levels in the TA of pre-symptomatic (P2) (**h**) and late-symptomatic (P7) (**i**) *Smn*^{-/-}
916 ;SMN2 mice and age-matched WT animals. Images are representative immunoblots. Data are mean ± SEM,
917 n = 3-4 animals per experimental group, unpaired t test, ns = not significant (**h**), p = 0.0215 (**i**). **j.** qPCR
918 analysis *NF-κB inducing kinase* (*NIK*) in TA muscle of late-symptomatic P7 *Smn*^{-/-};SMN2 and age-matched
919 WT animals. Data are mean ± SEM, n = 3-4 animals per experimental group, unpaired t test, p = 0.0094. **k-**
920 **q.** qPCR analysis of *parvalbumin* (**k**), *Tweak* (**l**), *Fn14* (**m**), *Pgc-1α* (**n**), *Mef2d* (**o**), *Glut-4* (**p**) and *HKII* (**q**)
921 in TA muscles from P0 (birth), P2 (pre-symptomatic), P4 (pre-symptomatic), P11 (early symptomatic) and
922 P19 (end-stage) *Smn*^{2B/-} and WT mice. Data are mean ± SEM, n = 3-4 animals per experimental group, two-
923 way ANOVA, Sidak's multiple comparison test, * p < 0.05, ** p < 0.01, *** p < 0.001, **** p < 0.0001.

924 **Figure 2. The TWEAK/Fn14 signaling pathway is not dysregulated in denervated muscles of pre-**
925 **weaned mice.** A sciatic nerve crush was performed on post-natal day (P) 7 WT FVB/N mice and both
926 ipsilateral (nerve crush) and contralateral (control) TA muscles were harvested at P14. **a.** Representative
927 images of hematoxylin and eosin-stained cross-sections of control and nerve crush TA muscles. Scale bars
928 = 100 μm. **b.** Myofiber area in control and nerve crush TA muscles. Data are mean ± SEM, n = 3-6 animals
929 per experimental group, unpaired t test, p = 0.0020. **c.** Myofiber size distribution in control and nerve crush
930 TA muscles. **d.** qPCR analysis of *parvalbumin*, *Tweak*, *Fn14*, *Pgc-1α*, *Mef2d*, *Glut-4*, *HKII*, *Klf15* and *Smn*

931 in control and nerve crush TA muscles. Data are mean \pm SEM, n = 4-6 animals per experimental group, two-
932 way ANOVA, uncorrected Fisher's LSD, ns = not significant.

933

934 **Figure 3. The TWEAK/Fn14 signaling pathway is dysregulated in cardiotoxin-induced muscle**
935 **necrosis in pre-weaned mice.** Cardiotoxin was injected in the left TA muscle of post-natal day (P) 10. The
936 right TA muscle was injected with equal volumes of 0.9% saline. TA muscles were harvested 6 days later.
937 **a.** Representative images of hematoxylin and eosin-stained cross-sections of saline- and cardiotoxin-injected
938 TA muscles. Scale bars = 100 μ m. **b.** Percentage of muscle fibers with centrally-located nuclei in saline- and
939 cardiotoxin-injected TA muscles. Data are mean \pm SEM, n = 3 animals per experimental group, unpaired *t*
940 test, *p* = 0.0020. **c.** qPCR analysis of *parvalbumin*, *Tweak*, *Fn14*, *Pgc-1a*, *Mef2d*, *Glut-4*, *HKII*, *Klf15* and
941 *Smn* in saline- and cardiotoxin-injected TA muscles. Data are mean \pm SEM, n = 3 animals per experimental
942 group, two-way ANOVA, uncorrected Fisher's LSD, ns = not significant, * *p* < 0.05, *** *p* < 0.001, **** *p*
943 < 0.0001.

944

945 **Figure 4. *Smn*, *Tweak* and *Fn14* depletion impact each other's expression and that of the Tweak/Fn14**
946 **signaling pathway. a-b.** qPCR analysis of *parvalbumin*, *Tweak*, *Fn14*, *Pgc-1a*, *Mef2d*, *Glut-4*, *HKII*, *Klf15*
947 and *Smn* in triceps muscle from post-natal day (P) 7 *Tweak*^{-/-} (**a**) and *Fn14*^{-/-} (**b**) mice. Data are mean \pm SEM,
948 n = 4 animals per experimental group, two-way ANOVA, uncorrected Fisher's LSD, ns = not significant, *
949 *p* < 0.05, *** *p* < 0.001, **** *p* < 0.0001. **c-j.** qPCR analysis of *Smn* (**c**), *Tweak* (**d**), *Fn14* (**e**), *Pgc-1a* (**f**),
950 *Mef2d* (**g**), *Glut-4* (**h**), *HKII* (**i**) and *Klf15* (**j**) in siRNA-mediated *Tweak*-, *Fn14*- and *Smn*-depleted and
951 control proliferating (Day 0) and differentiated (Day 7) C2C12 cells. Data are mean \pm SEM, n = 3 per
952 experimental group, two-way ANOVA, Dunnett's multiple comparisons test, * *p* < 0.05, ** *p* < 0.01, *** *p*
953 < 0.001, **** *p* < 0.0001. **k.** Proposed model of the relationship between *Smn* and the Tweak/Fn14 signaling
954 pathway. Red lines represent inhibition and blue lines represent activation.

955

956 **Figure 5. Overlap between dysregulated genes involved in myopathy, myogenesis and glucose**
957 **metabolism in skeletal muscle of *Smn*^{-/-};SMN2, *Fn14*^{-/-} and *Tweak*^{-/-} mice. a.** Venn diagram showing
958 overlap of genes involved in myopathy and myogenesis that are significantly dysregulated in the same
959 direction (either up or downregulated, $p < 0.05$) in triceps and quadriceps muscle from post-natal day (P) 7
960 compared to *Smn*^{-/-};SMN2, *Fn14*^{-/-} and *Tweak*^{-/-} mice to age- and genetic strain-matched wild type (WT)
961 mice. **b.** Network and enrichment analysis of the overlap of significantly dysregulated myopathy and
962 myogenesis genes in triceps and/or quadriceps of P7 *Smn*^{-/-};SMN2, *Fn14*^{-/-} and *Tweak*^{-/-} mice using STRING
963 software. Smn (Smn1), TWEAK (Tnfsf12) and Fn14 (Tnfrsf12a) are included in the analysis. Corresponding
964 protein nodes in the network are highlighted in color. The connection color and shape between proteins
965 represent protein-protein associations (Action types) and if the association is positive, negative or
966 unspecified (Action effects). **c.** Venn diagram showing overlap of genes involved in glucose metabolism that
967 are significantly dysregulated in the same direction (either up or downregulated, $p < 0.05$) in triceps and
968 quadriceps muscle from P7 compared to *Smn*^{-/-};SMN2, *Fn14*^{-/-} and *Tweak*^{-/-} mice to age- and genetic strain-
969 matched WT mice. **d.** Network and enrichment analysis of the overlap of significantly dysregulated
970 myopathy and myogenesis genes in triceps and/or quadriceps of P7 *Smn*^{-/-};SMN2, *Fn14*^{-/-} and *Tweak*^{-/-} mice
971 using STRING software. Smn (Smn1), TWEAK (Tnfsf12), Fn14 (Tnfrsf12a), HKII (Hk2), Glut4 (Slc2a4),
972 Pgc-1 α (Ppargc1a), Klf15 and Mef2d are included in the analysis. Corresponding protein KEGG pathways
973 with the six lowest FDRs highlighted in color (see Table 3). The connection color and shape between proteins
974 represent protein-protein associations (Action types) and if the association is positive, negative or
975 unspecified (Action effects).

976

977 **Figure 6. Increasing Tweak activity via Fc-TWEAK improves disease phenotypes in two SMA mouse**
978 **models. a.** Daily weights of untreated *Smn*^{-/-};SMN2 SMA mice and *Smn*^{-/-};SMN2 mice that received daily
979 subcutaneous injections (starting at P0) of Fc-TWEAK or IgG control (15.8 μ g). Data are mean \pm SEM, $n =$
980 7-10 animals per experimental group, two-way ANOVA, Sidak's multiple comparison test. **b.** Survival

981 curves of untreated *Smn*^{-/-};SMN2 SMA mice and *Smn*^{-/-};SMN2 that received daily subcutaneous injections of
982 Fc-TWEAK or IgG control (15.8 µg). Data are represented as Kaplan-Meier survival curves, n = 7-10
983 animals per experimental group, Log-rank (Mantel-Cox). **c-i.** qPCR analysis of *Tweak* (**c**), *Fn14* (**d**), *Pgc-1α* (**e**), *Mef2d* (**f**), *Glut-4* (**g**), *HKII* (**h**) and *Klf15* (**i**) in triceps of post-natal day (P) 7 untreated and Fc-
985 TWEAK-treated (15.8 µg) *Smn*^{-/-};SMN2 SMA and *Smn*^{+/+};SMN2 health littermates. Data are mean ± SEM,
986 n = 3-4 animals per experimental group, two-way ANOVA, uncorrected Fisher's LSD, * p < 0.05, *** p
987 <0.001. **j.** Representative images of laminin-stained cross-sections of TA muscles from P7 untreated and Fc-
988 TWEAK-treated (15.8 µg) *Smn*^{-/-};SMN2 SMA and *Smn*^{+/+};SMN2 health littermates. Scale bars = 100 µm. **k.**
989 Quantification of myofiber area in the TAs of P7 untreated and Fc-TWEAK-treated (15.8 µg) *Smn*^{-/-};SMN2
990 SMA and *Smn*^{+/+};SMN2 health littermates. Data are mean ± SEM, n = 3-4 animals per experimental group
991 (>550 myofibers per experimental group), two-way ANOVA, Tukey's multiple comparison test, * p < 0.05,
992 **** p < 0.0001. **l.** Relative frequency distribution of myofiber size in TA muscles of P7 untreated and
993 Fc-TWEAK-treated (15.8 µg) *Smn*^{-/-};SMN2 SMA and *Smn*^{+/+};SMN2 health littermates. **m-r.** qPCR analysis
994 of *parvalbumin* (**m**), *MuRF-1* (**n**), *atrogin-1* (**o**), *Myod1* (**p**), and *myogenin* (**r**) in triceps of P7 untreated and
995 Fc-TWEAK-treated (15.8 µg) *Smn*^{-/-};SMN2 SMA and *Smn*^{+/+};SMN2 health littermates. Data are mean ±
996 SEM, n = 3-4 animals per experimental group, two-way ANOVA, uncorrected Fisher's LSD, * p < 0.05, **
997 p <0.01. **s.** Daily weights of untreated *Smn*^{2B/-} SMA mice and *Smn*^{2B/-} mice that received subcutaneous
998 injections of Fc-TWEAK or IgG control (15.8 µg) every 4 days (starting at P0). Data are mean ± SEM, n =
999 9-12 animals per experimental group, two-way ANOVA, Sidak's multiple comparison test. **t.** Survival
1000 curves of untreated *Smn*^{2B/-} SMA mice and *Smn*^{2B/-} mice that received subcutaneous injections of Fc-TWEAK
1001 or IgG control (15.8 µg) every 4 days (starting at P0). Data are Kaplan-Meier survival curves, n = 9-12
1002 animals per experimental group, Log-rank (Mantel-Cox), p = 0.0162. **u.** qPCR analysis of Glut-4 in P15
1003 *Smn*^{2B/-} SMA mice and *Smn*^{2B/-} mice that received subcutaneous injections of Fc-TWEAK or IgG control

1004 (15.8 μ g) every 4 days (starting at P0). Data are mean \pm SEM, n = 3-4 animals per experimental group, two-
1005 way ANOVA, uncorrected Fisher's LSD, * p < 0.05.
1006

1007 **TABLES**

1008 **Table 1.** Myogenesis and myopathy genes significantly dysregulated in the same direction in triceps and
1009 quadriceps of P7 *Smn*^{-/-}; *SMN2*, *Fn14*^{-/-} and *Tweak*^{-/-} mice when compared to P7 WT mice.

1010

1011 **Table 2.** Glucose metabolism genes significantly dysregulated in the same direction in triceps and
1012 quadriceps of P7 *Smn*^{-/-}; *SMN2*, *Fn14*^{-/-} and *Tweak*^{-/-} mice when compared to P7 WT mice.

1013

1014 **Table 3.** KEGG pathways generated from glucose metabolism genes that were significantly dysregulated
1015 in the same direction in triceps and quadriceps of P7 *Smn*^{-/-}; *SMN2*, *Fn14*^{-/-} and *Tweak*^{-/-} mice when compared
1016 to P7 WT mice.

1017

1018 **SUPPLEMENTARY FIGURE LEGENDS**

1019 **Supplementary Figure 1. Effect of varying Fc-TWEAK on disease progression in *Smn*^{-/-};SMN2 SMA**
1020 **mice.** *Smn*^{-/-};SMN2 mice received daily subcutaneous injections of increasing doses of Fc-TWEAK (7.9, 15.,
1021 23.7 and 31.6 µg), starting at birth. **a.** Daily weights of untreated *Smn*^{-/-};SMN2 SMA mice and *Smn*^{-/-};SMN2
1022 mice that received daily subcutaneous injections (starting at P0) of Fc-TWEAK (7.9, 15.8, 23.7 and 31.6
1023 µg). Data are mean ± SEM, n = 5-10 animals per experimental group, two-way ANOVA, Sidak's multiple
1024 comparison test. **b.** Survival curves of untreated *Smn*^{-/-};SMN2 SMA mice and *Smn*^{-/-};SMN2 mice that
1025 received daily subcutaneous injections (starting at P0) of Fc-TWEAK (7.9, 15.8, 23.7 and 31.6 µg). Data are
1026 presented as Kaplan-Meier survival curves, n = 5-10 animals per experimental group, Log-rank (Mantel-
1027 Cox).

1028

1029 **SUPPLEMENTARY TABLES**

1030

1031 **Supplementary Table 1. Mouse primers used for quantitative real-time PCR.**

1032

1033

1034

1035

1036

1037

1038

1039

1040

1041

1042

1043

1044

1045

1046

1047

1048

1049

1050

1051

1052

1053

1054 **SUPPLEMENTARY FILES**

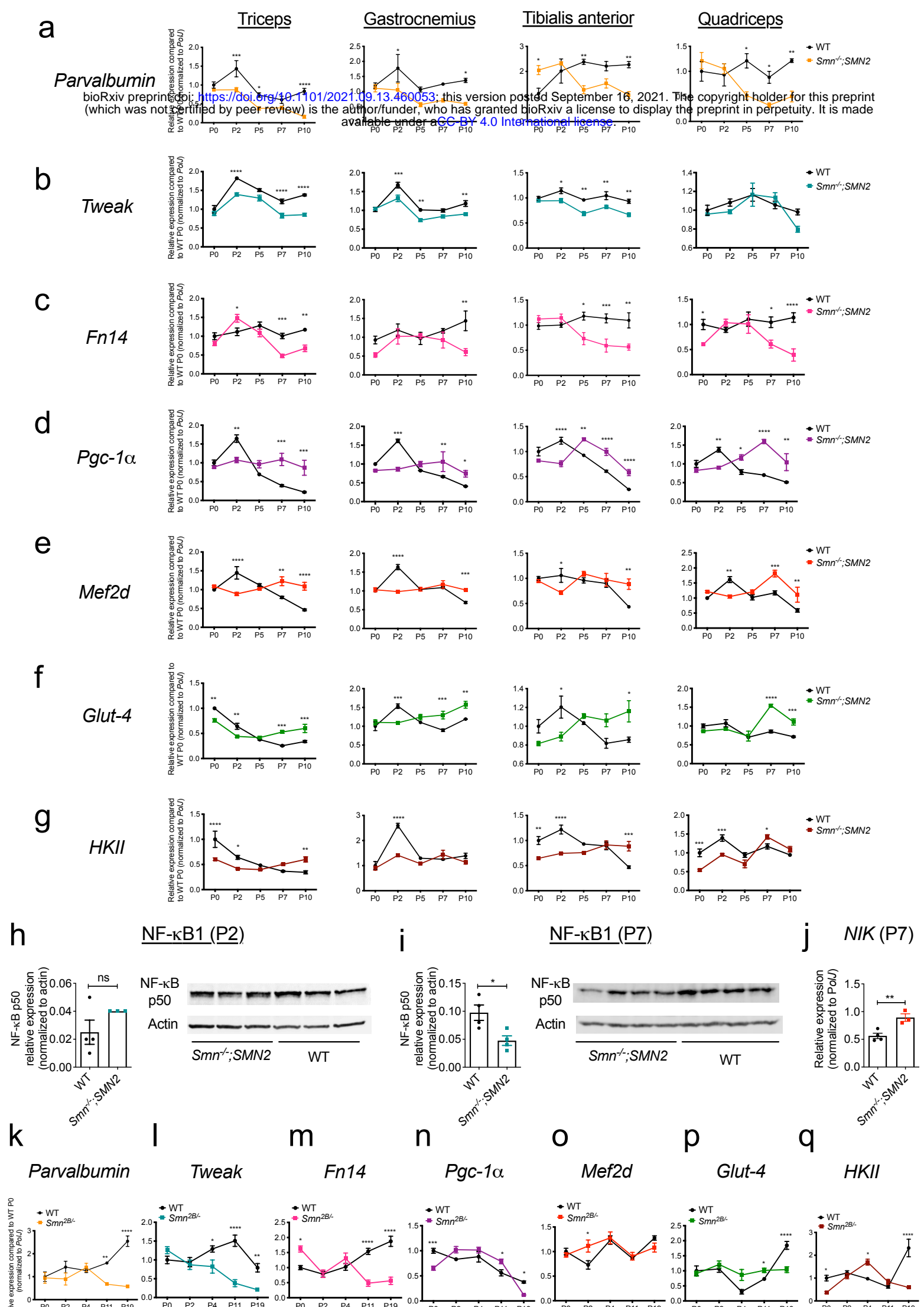
1055 **Supplementary File 1.** Myopathy and myogenesis gene expression changes in triceps and quadriceps
1056 of post-natal day 7 *Smn*^{-/-};SMN2 (SMA), *Tweak*^{-/-} (Tweak KO) and *Fn14*^{-/-}; (Fn14 KO) compared to
1057 age- and genetic strain-matched wild type animals.

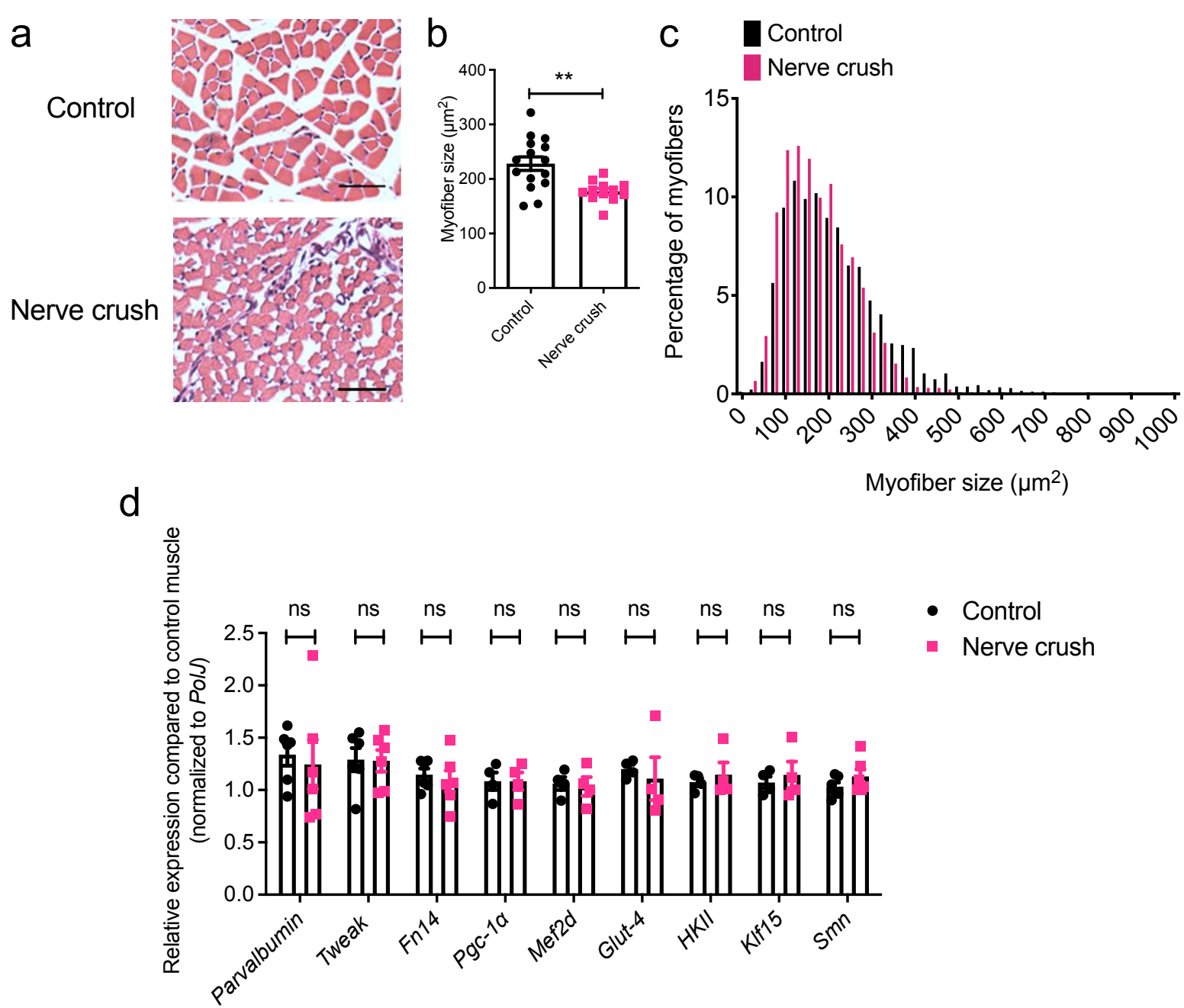
1058

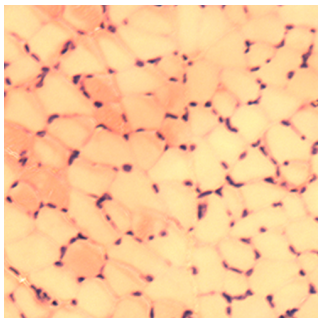
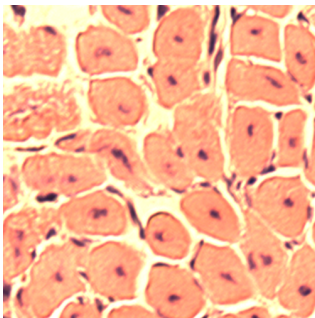
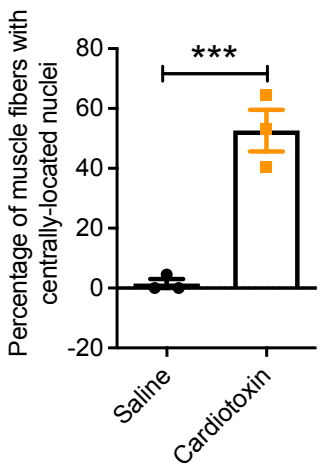
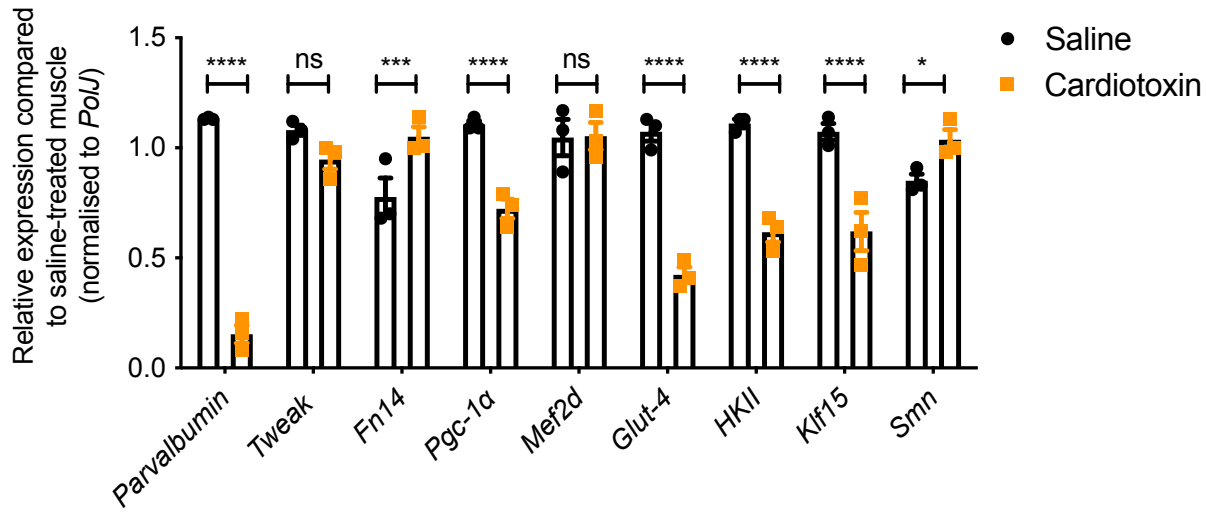
1059 **Supplementary File 2.** Glucose metabolism gene expression changes in triceps and quadriceps
1060 of post-natal day 7 *Smn*^{-/-};SMN2 (SMA), *Tweak*^{-/-} (Tweak KO) and *Fn14*^{-/-}; (Fn14 KO) compared to age-
1061 and genetic strain-matched wild type animals.

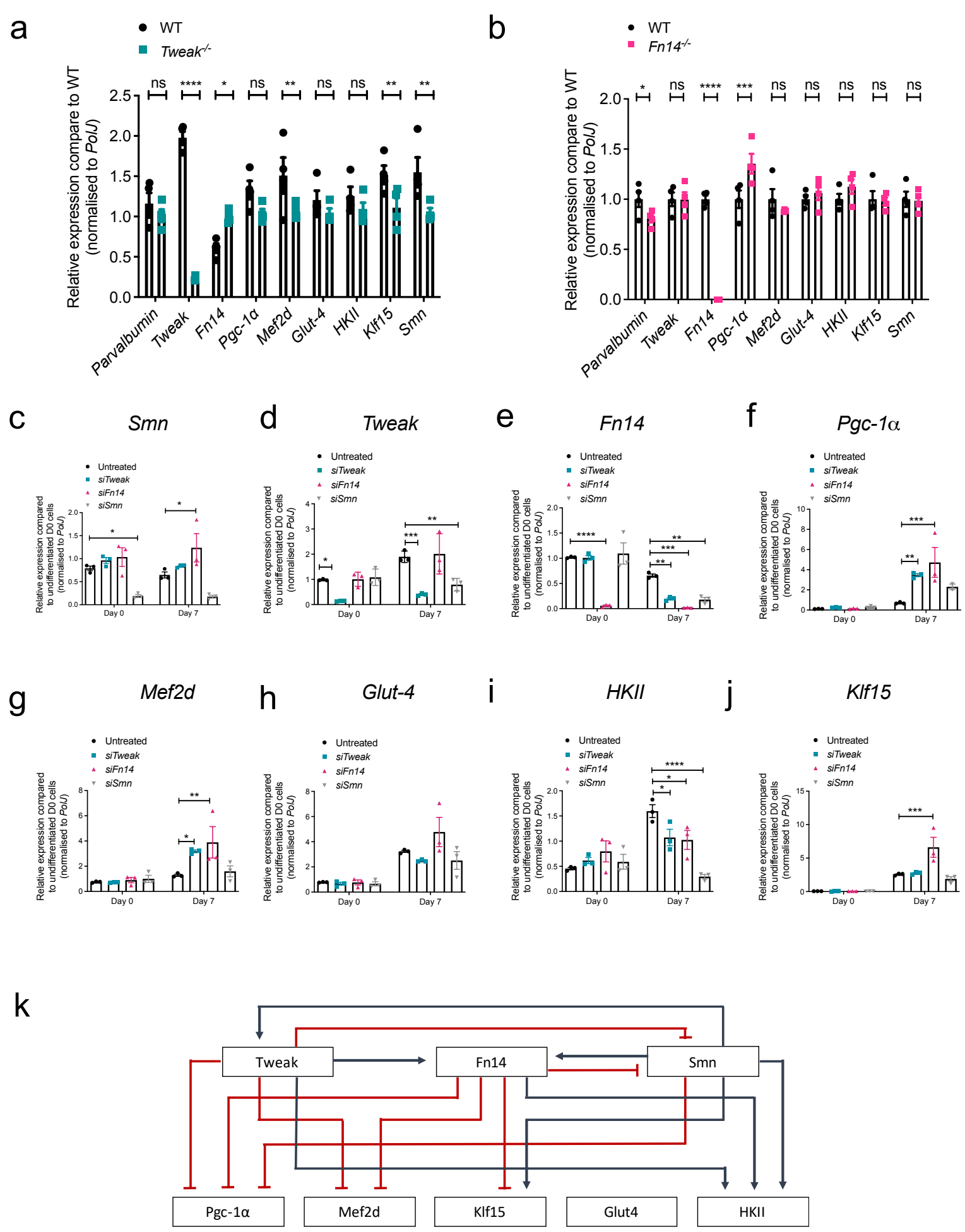
1062

1063





a Saline**a** Cardiotoxin**b****c**

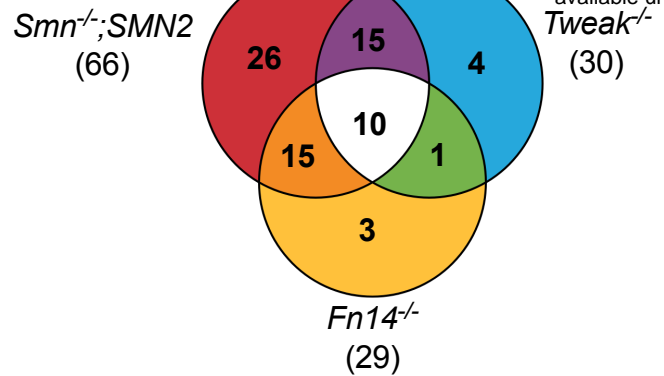
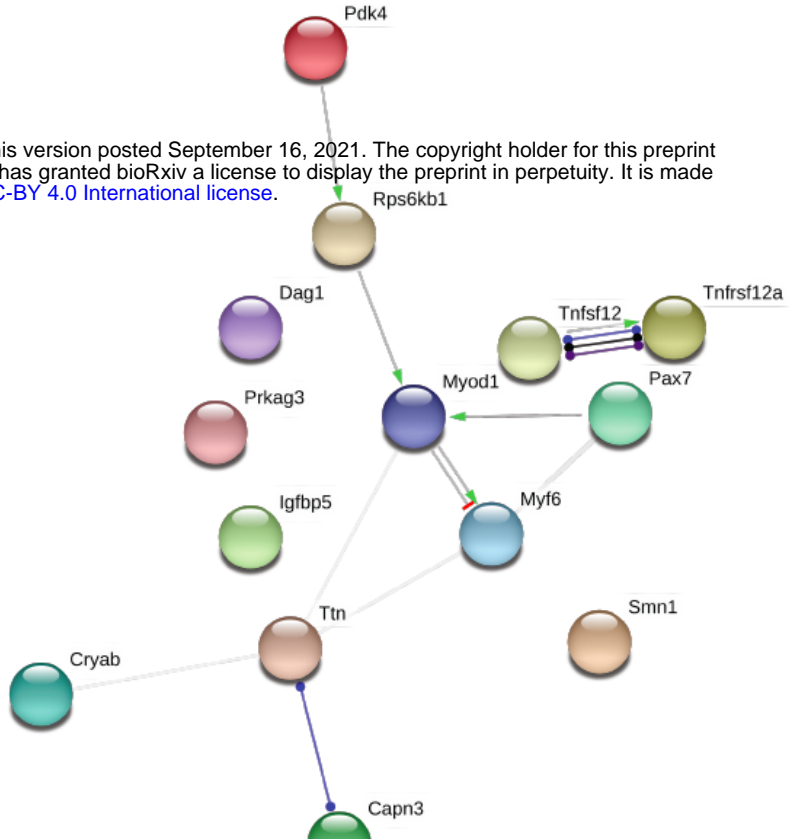
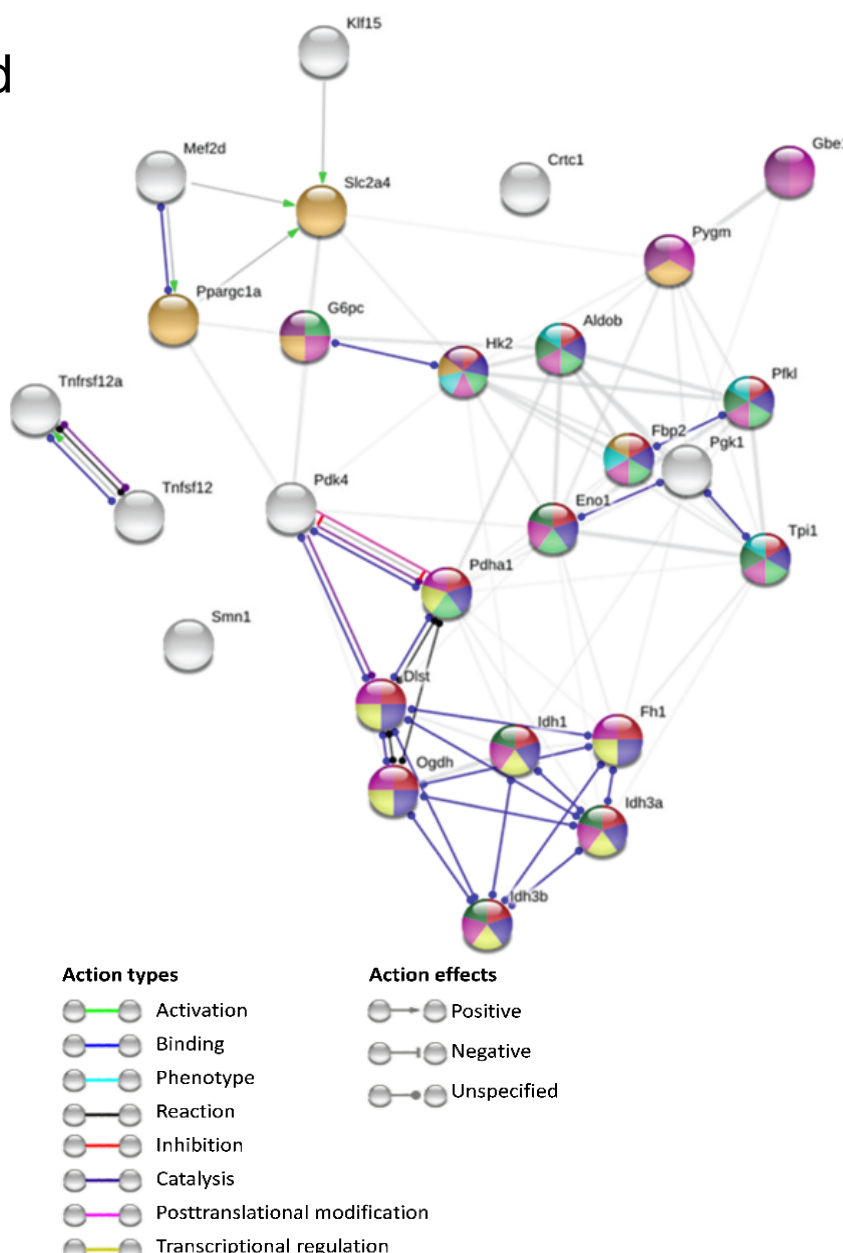


a

Myopathy and myogenesis

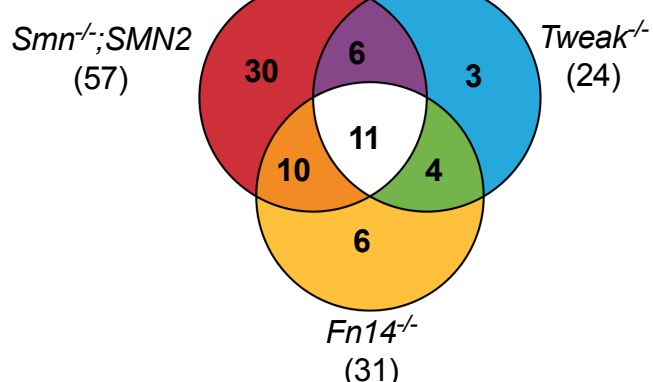
Triceps

bioRxiv preprint doi: <https://doi.org/10.1101/2021.09.13.460053>; this version posted September 16, 2021. The copyright holder for this preprint (which was not certified by peer review) is the author/funder, who has granted bioRxiv a license to display the preprint in perpetuity. It is made available under aCC-BY 4.0 International license.

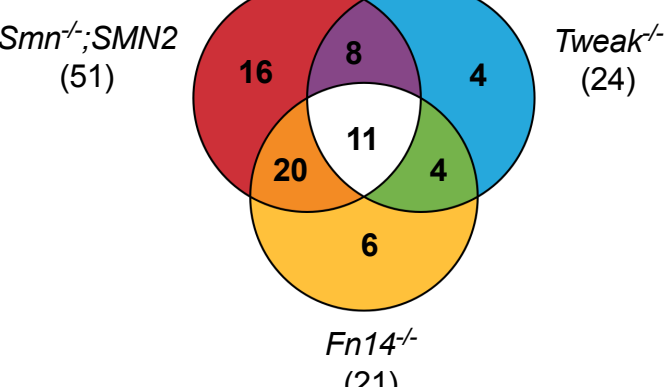
**b****d****c**

Glucose metabolism

Triceps



Quadriceps



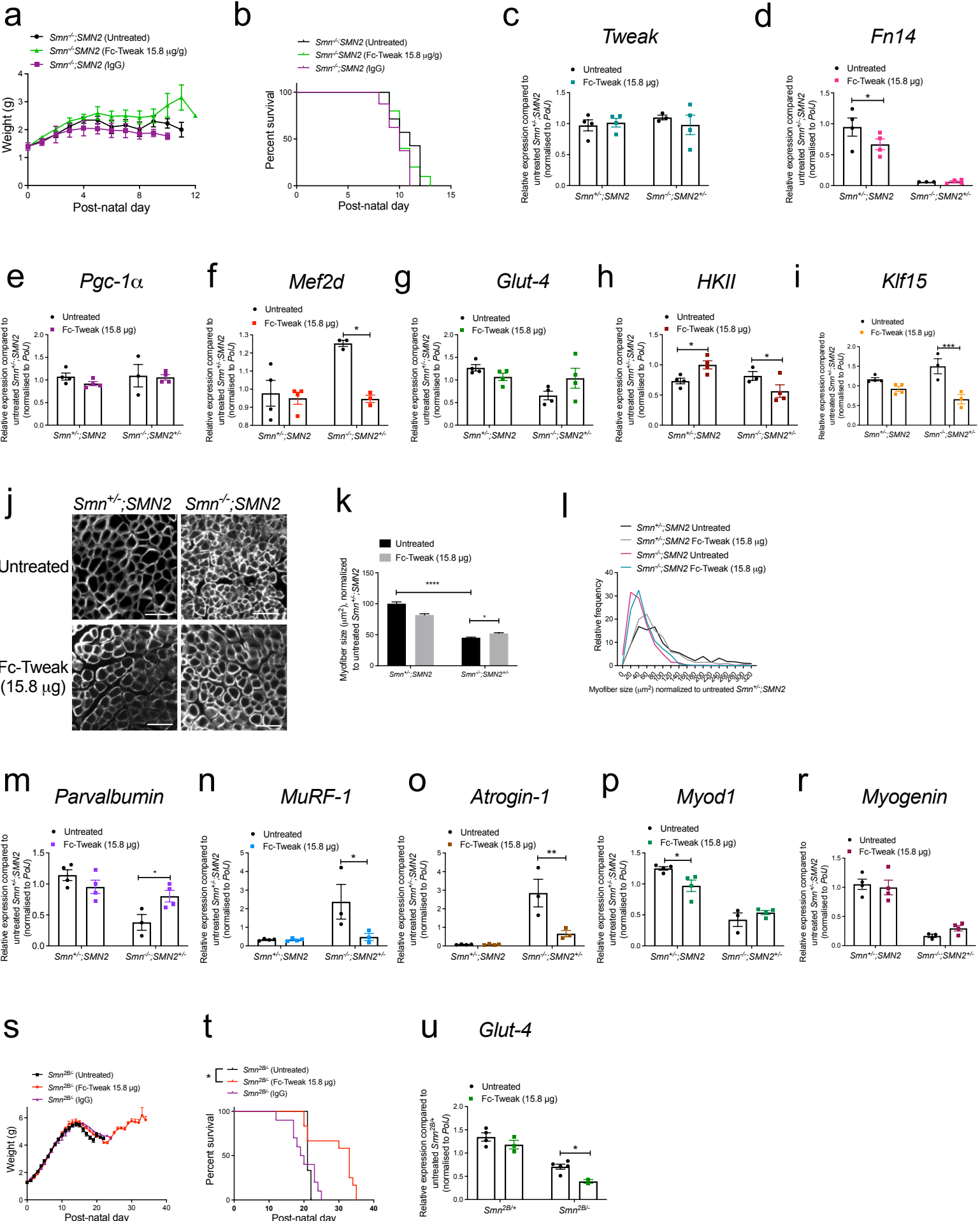


Table 1. Myogenesis and myopathy genes significantly dysregulated in the same direction in triceps and quadriceps of P7 *Smn*^{-/-};SMN2, *Fn14*^{-/-} and *Tweak*^{-/-} mice when compared to P7 WT mice.

Gene	Triceps	Quadriceps
<i>Calpain3</i> (Capn3)	Up	Up
<i>Crystallin Alpha B</i> (Cryab)	Up	—
<i>Dystroglycan 1</i> (Dag1)	Down	Down
<i>Insulin Like Growth Factor Binding Protein 5</i> (Igfbp5)	Down	—
<i>Myogenic Factor 6</i> (Myf6)	Up	—
<i>Myogenic Differentiation 1</i> (Myod1)	Up	—
<i>Paired Box 7</i> (Pax7)	Down	—
<i>Protein Kinase AMP-Activated Non-Catalytic Subunit Gamma 3</i> (Prkag3)	Down	Down
<i>Pyruvate Dehydrogenase Kinase 4</i> (Pdk4)	Up	—
<i>Ribosomal Protein S6 Kinase B1</i> (Rps6kb1)	Down	Down
<i>Titin</i> (Ttn)	—	Down

Table 2. Glucose metabolism genes significantly dysregulated in the same direction in triceps and quadriceps of P7 *Smn*^{-/-};SMN2, *Fn14*^{-/-} and *Tweak*^{-/-} mice when compared to P7 WT mice.

Gene	<i>Triceps</i>	<i>Quadriceps</i>
<i>Aldolase, Fructose-Bisphosphate B</i> (Aldob)	Down	—
<i>1,4-Alpha-Glucan Branching Enzyme 1</i> (Gbe1)	—	Down
<i>Dihydrolipoamide S-Succinyltransferase</i> (Dlst)	Down	Down
<i>Enolase 1</i> (Enol)	Down	Down
<i>Filamin B</i> (Fh1)	Down	—
<i>Fructose-Bisphosphatase 2</i> (Fbp2)	Up	—
<i>Glucose-6-Phosphatase Catalytic Subunit</i> (G6pc)	Down	—
<i>Glycogen Phosphorylase Muscle Associated</i> (Pygm)	—	Down
<i>Isocitrate Dehydrogenase (NADP(+)) 1, Cytosolic</i> (Idh1)	Down	—
<i>Isocitrate Dehydrogenase 3 (NAD(+)) Alpha</i> (Idh3a)	Down	Down
<i>Isocitrate Dehydrogenase 3 (NAD(+)) Beta</i> (Idh3b)	—	Down
<i>Oxoglutarate Dehydrogenase</i> (Ogdh)	Down	Down
<i>Phosphofructokinase, Liver Type</i> (Pfkl)	—	Down
<i>Pyruvate Dehydrogenase E1 Alpha 1 Subunit</i> (Pdha1)	—	Down
<i>Pyruvate Dehydrogenase Kinase 4</i> (Pdk4)	Up	Up
<i>Phosphoglycerate Kinase 1</i> (Pgk1)	Down	—
<i>Triosephosphate Isomerase 1</i> (Tpi1)	—	Down

Table 3. KEGG pathways generated from glucose metabolism genes that were significantly dysregulated in the same direction in triceps and quadriceps of P7 *Smn*^{-/-}; *SMN2*, *Fn14*^{-/-} and *Tweak*^{-/-} mice when compared to P7 WT mice.

Pathway ID	Pathway description	Count in gene set	False discovery rate (FDR)
01200	Carbon metabolism	13	7.62e-22
01120	Microbial metabolism in diverse environments	13	1.87e-19
00010	Glycolysis/Gluconeogenesis	8	2.09e-13
00020	Citrate cycle (TCA cycle)	7	2.09e-13
01100	Metabolic pathways	16	7.65e-13
01230	Biosynthesis of amino acids	7	8.75e-11
00051	Fructose and mannose metabolism	5	1.7e-08
04910	Insulin signaling pathway	6	3.09e-07
00500	Starch and sucrose metabolism	4	8.58e-06
04152	AMPK signaling pathway	5	8.58e-06
01210	2-Oxocarboxylic acid metabolism	3	2.79e-05
00030	Pentose phosphate pathway	3	0.000126
04066	HIF-1 signaling pathway	4	0.000141
00052	Galactose metabolism	3	0.000145
04920	Adipocytokine signaling pathway	3	0.00138
00620	Pyruvate metabolism	2	0.0177
04973	Carbohydrate digestion and absorption	2	0.0177
04930	Type II diabetes mellitus	2	0.0227
00310	Lysine degradation	2	0.0233